AMERICAN SOCIETY FOR MICROBIOLOGY | Applied and Environmental Microbiology®

GEOMICROBIOLOGY

Microaerophilic Fe(II)-Oxidizing *Zetaproteobacteria* Isolated from Low-Fe Marine Coastal Sediments: Physiology and Composition of Their Twisted Stalks

K. Laufer,[a]* M. Nordhoff,[a] M. Halama,[a] R. E. Martinez,[b] M. Obst,[c] M. Nowak,[d] H. Stryhanyuk,[e] H. H. Richnow,[e] A. Kappler[a,f]

Geomicrobiology, Center for Applied Geosciences, University of Tübingen, Tübingen, Germany[a]; Mineralogy-Petrology, Institute of Environmental Sciences, University of Freiburg, Freiburg im Breisgau, Germany[b]; Experimental Biogeochemistry, Bayreuth Center for Ecology and Environmental Research, University of Bayreuth, Bayreuth, Germany[c]; Experimental Mineralogy, Mineralogy and Geodynamics, University of Tübingen, Tübingen, Germany[d]; ProVIS, Centre for Chemical Microscopy, Helmholtz Centre for Environmental Research (UFZ), Leipzig, Germany[e]; Center for Geomicrobiology, Department of Bioscience, Aarhus University, Aarhus, Denmark[f]

ABSTRACT Microaerophilic Fe(II) oxidizers are commonly found in habitats containing elevated Fe(II) and low O_2 concentrations and often produce characteristic Fe mineral structures, so-called twisted stalks or tubular sheaths. Isolates originating from freshwater habitats are all members of the *Betaproteobacteria*, while isolates from marine habitats belong almost exclusively to the *Zetaproteobacteria*. So far, only a few isolates of marine microaerophilic Fe(II) oxidizers have been described, all of which are obligate microaerophilic Fe(II) oxidizers and have been thought to be restricted to Fe-rich systems. Here, we present two new isolates of marine microaerophilic Fe(II)-oxidizing *Zetaproteobacteria* that originate from typical coastal marine sediments containing only low Fe concentrations (2 to 11 mg of total Fe/g of sediment [dry weight]; 70 to 100 μM dissolved Fe^{2+} in the porewater). The two novel *Zetaproteobacteria* share characteristic physiological properties of the *Zetaproteobacteria* group, even though they come from low-Fe environments: the isolates are obligate microaerophilic Fe(II) oxidizers and, like most isolated *Zetaproteobacteria*, they produce twisted stalks. We found a low organic carbon content in the stalks (~0.3 wt%), with mostly polysaccharides and saturated aliphatic chains (most likely lipids). The Fe minerals in the stalks were identified as lepidocrocite and possibly ferrihydrite. Immobilization experiments with Ni^{2+} showed that the stalks can function as a sink for trace metals. Our findings show that obligate microaerophilic Fe(II) oxidizers belonging to the *Zetaproteobacteria* group are not restricted to Fe-rich environments but can also be found in low-Fe marine environments, which increases their overall importance for the global biogeochemical Fe cycle.

IMPORTANCE So far, only a few isolates of benthic marine microaerophilic Fe(II) oxidizers belonging to the *Zetaproteobacteria* exist, and most isolates were obtained from habitats containing elevated Fe concentrations. Consequently, it was thought that these microorganisms are important mainly in habitats with high Fe concentrations. The two novel isolates of *Zetaproteobacteria* that are presented in the present study were isolated from typical coastal marine sediments that do not contain elevated Fe concentrations. This increases the knowledge about possible habitats in which *Zetaproteobacteria* can exist. Furthermore, we show that the physiology and the typical organo-mineral structures (twisted stalks) that are produced by the isolates do not notably differ from the physiology and the cell-mineral structures of

Received 11 November 2016 **Accepted** 28 January 2017

Accepted manuscript posted online 3 February 2017

Citation Laufer K, Nordhoff M, Halama M, Martinez RE, Obst M, Nowak M, Stryhanyuk H, Richnow HH, Kappler A. 2017. Microaerophilic Fe(II)-oxidizing *Zetaproteobacteria* isolated from low-Fe marine coastal sediments: physiology and composition of their twisted stalks. Appl Environ Microbiol 83:e03118-16. https://doi.org/10.1128/AEM.03118-16.

Editor Joel E. Kostka, Georgia Institute of Technology

Address correspondence to A. Kappler, andreas.kappler@uni-tuebingen.de.

* Present address: K. Laufer, Center for Geomicrobiology, Department of Bioscience, Aarhus University, Aarhus, Denmark.

K. Laufer and M. Nordhoff contributed equally to this article.

isolates from environments with high Fe concentrations. We also showed that the organo-mineral structures can function as a sink for trace metals.

KEYWORDS geomicrobiology, iron oxidizers, marine microbiology, sediment

The characteristic organo-mineral structures that are produced by most microaerophilic Fe(II)-oxidizing bacteria were first described in 1836 by Ehrenberg (1). It took more than 70 years before these bacteria were cultivated in the laboratory (2), which remains challenging, due to their specific requirements regarding oxygen and Fe(II) concentrations. At circumneutral pH, at which these bacteria live, they have to compete with the abiotic oxidation of Fe(II) by O_2 (3, 4). At low O_2 concentrations, this abiotic reaction is slow and the bacteria are able to outcompete the abiotic reaction (5, 6).

Microaerophilic Fe(II) oxidizers are commonly found in environments where opposing gradients of O_2 and Fe(II) exist (7). They have been found in freshwater habitats, such as wetland sediments and Fe(II)-rich springs (8–11), as well as in marine habitats, including sediments from a continental margin (12), hydrothermal vents (13–16), coastal seawater (17, 18), and in a redox-stratified water column (19). So far, microaerophilic Fe(II) oxidizers from marine habitats almost exclusively belong to the *Zetaproteobacteria* (20, 21). One exception was reported in a study by Edwards et al. (13), who isolated psychrophilic microaerophilic Fe(II) oxidizers related to the *Alphaproteobacteria* and *Gammaproteobacteria*. All known isolates of the *Zetaproteobacteria* are obligate microaerophilic Fe(II)-oxidizing bacteria which belong to the genus *Mariprofundus*. However, the number of isolates is very limited and probably not representative of the diversity of *Zetaproteobacteria*. So far, six isolates were described, and four of these were isolated from Fe mats at the Lō'ihi Seamount hydrothermal vents, Hawaii, USA (9, 20, 22, 23). More isolates originated from an Fe mat in a salt marsh in Maine, USA (17) and the oxic-anoxic boundary layer at the redox-stratified water column of Chesapeake Bay (19).

Based on molecular data, there is evidence for the worldwide presence of *Zetaproteobacteria* (Fig. 1). The majority of studies on microaerophilic Fe(II)-oxidizing bacteria were performed in habitats with elevated aqueous and solid-phase Fe(II) concentrations, and to date, all benthic isolates were obtained from such habitats. These habitats include Fe mats at hydrothermal vents or Fe-rich seeps in salt marshes, with an Fe content of up to 183 mg/g of sediment (dry weight) (24), which we refer to as high-Fe environments. So far, no isolates were obtained from typical marine sediments with an Fe content in the low-milligram to gram range, such as those from which the isolates were obtained in the present study (2 to 11 mg/g of sediment [dry weight]) (25). We refer to these environments as low-Fe environments, relative to the high-Fe environments defined above. However, the primary requirement for their growth, i.e., an interface of redox gradients of Fe and oxygen, is common in the environment and is typical of marine sediments. Porewater concentrations of Fe(II) in these sediments range from tens to hundreds micromolar (26) and are potentially suitable for the growth of marine microaerophilic Fe(II) oxidizers (27, 28). In a previous study, we found evidence for the presence of *Zetaproteobacteria* in these sediments using the cultivation-dependent most probable number (MPN) technique (up to 1×10^6 cells · g of sediment^{-1} [dry weight]) and quantitative PCR (qPCR) (up to 3.2×10^6 cells · g of sediment^{-1} [dry weight]) (25).

Most known marine *Zetaproteobacteria* have been shown to produce organo-mineral structures in the form of either twisted stalks or tubular sheaths, with lengths of several micrometers to tens of micrometers, similar to many microaerophilic Fe(II)-oxidizing bacteria from freshwater habitats (22, 29, 30). Mineralogical analyses of the biogenic minerals in twisted stalks formed by *Zetaproteobacteria* identified mainly a remarkably stable, poorly crystalline ferrihydrite (29, 31). In one of these studies, lepidocrocite was found at the surface of stalks (29). Spectroscopic and microscopic analyses of the organic components present in twisted stalks from marine and freshwater microaerophilic Fe(II)-oxidizing bacteria indicated the presence of acidic poly-

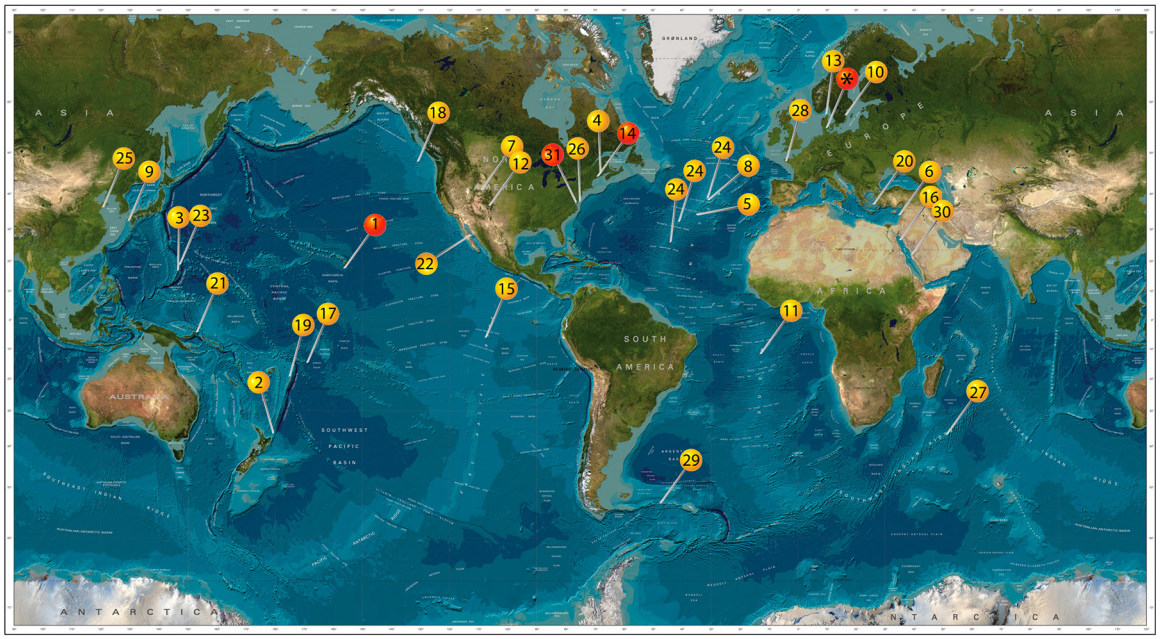

FIG 1 World map showing locations where evidence for the presence of *Zetaproteobacteria* is present based on molecular data (yellow pins) and where in addition to molecular data isolates are also present (red pins). 1, Lō'ihi Seamount (14, 20, 22, 24, 30, 58, 74, 75); 2, Kermandec Arc (76); 3, Southern Mariana Trough (16, 77, 78); 4, Sheepscot River, Maine, USA (50); 5 and 8, Mid-Atlantic Ridge (79, 80); 6, Levantine basin, (12); 7, Crystal Geyser, Utah, USA (81); 9, Nagahama Bay (57); 10, Äspö Hard Rock Laboratory (82); 11, South Mid-Atlantic Ridge (83); 12, springs in New Mexico, USA (84); 13, Skagerrak (49); 14, Boothbay Harbor, Maine, USA (17); 15, East Pacific Rise (85); 16, Kebrit Deep, Red Sea (86); 17, Vailulu'u Seamount (87); 18, Juan de Fuca Ridge (88, 89); 19, Tonga Arc (15); 20, Nea Kameni Island, Greece (90); 21, Tutum Bay, Ambitle Island (91); 22, Southern Guyamas vent field (92); 23, Southern Mariana Trench (93); 24, Mid-Atlantic Ridge (various sites) (21); 25, Quingdao coastal waters (18); 26, beach aquifer, Cape Shores, Lewes, Delaware, USA (94); 27, Indian Ridge (95); 28, tidal basin Aber-Benoit, Treglonou, France (96); 29, surface water between the Polar Front and the Southern Antarctic Circumpolar Current in the Southern Ocean (97); 30, water desalination plant in Saudi Arabia (98); 31 Chesapeake Bay, USA (19); *, Aarhus Bay (this study). This image builds upon previous work by McAllister et al. (20). (Image reproduced from the GEBCO world map, 2014 [www.gebco.net].)

saccharides, saturated lipids, and a small amount of protein (29, 32–35). However, more detailed information on the exact nature of these organic compounds is so far lacking. Chan et al. (29) described a model for Fe(II) oxidation by the marine microaerophilic Fe(II) oxidizer *Mariprofundus ferrooxydans* PV-1 in which cells excrete oxidized Fe, i.e., Fe(III), from discrete locations on the cell surface bound to organic polymers that then become the fibers of the twisted stalks. The authors provide evidence that precipitation of the Fe(III) bound to the organic polymers only starts to occur over time within the stalks and thereby is directed away from the cell. A later study (35) found evidence that stalks of *Mariprofundus ferrooxydans* PV-1 might contain a much lower fraction of organic carbon than previously thought. The authors found hints of evidence that adsorption of cellular material released during osmotic shock introduced by sample preparation may be responsible for higher fractions of organic carbon in the stalks (35). Such sorption of charged organic molecules, but also binding of metal cations, such as nickel, to the stalks, is expected based on previous studies with microaerophilic (31, 34–37) and anaerobic Fe(II)-oxidizing bacteria (34, 38–41). Some of these metal cations are important for bacterial growth (42, 43); nickel, for example, is an essential nutrient for some microorganisms and is incorporated into nickel-dependent enzymes (43). Binding of nickel to stalks therefore can affect its availability to microorganisms. This has been reported for microaerophilic bacteria from an abandoned silver mine (34). In marine environments, nickel was found in biogenic iron oxide deposits at a hydrothermal vent (44) that contained sheaths and stalks produced by microaerophilic bacteria but also other components, like diatoms and organic carbon. However, specific information about how twisted stalks in particular affect nickel availability in marine systems is missing.

Based on the knowledge gaps described above, the aim of this study was to characterize two isolates of microaerophilic Fe(II)-oxidizing microorganisms from typi-

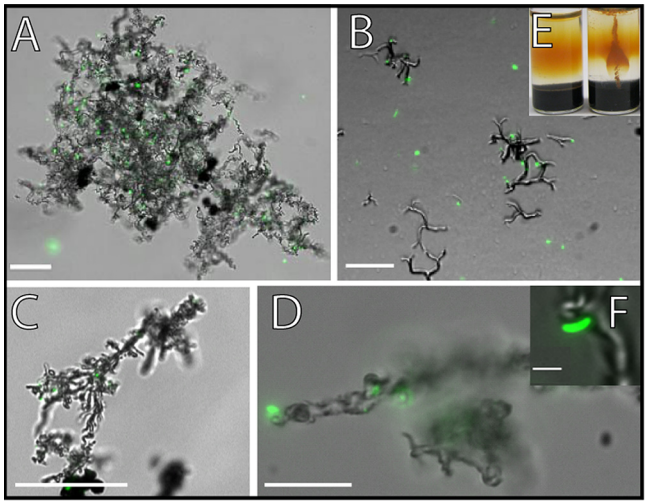

FIG 2 Overlay of fluorescence and transmission light microscopic pictures of the microaerophilic Fe(II) oxidizers that were isolated in this study (A to D and F) and a picture of a culture growing in a gradient tube (E). Cells were stained with the LIVE/DEAD stain. Only the green fluorescence as seen with the filter set L5 is shown. (A, B, and F) Culture that was isolated from Norsminde Fjord, grown on ZVI plates (A) and in gradient tubes (B). (C and D) Culture from Kalø Vig, both grown on ZVI plates. Scale bars: 25 μm (A to C), 10 μm (D), and 1 μm (F). (E) Uninoculated gradient tube on the left and on the right a gradient tube that was inoculated with the culture from Norsminde Fjord. Panels A and F reprinted from reference 25.

cal coastal marine sediments (Norsminde Fjord and Kalø Vig, Denmark). The specific goals were to (i) evaluate the phylogenetic and physiological properties of the isolated bacteria, as well as their potential contribution to autotrophic Fe(II) oxidation in low-Fe environments, (ii) determine the properties of the twisted stalks (structure, mineralogy, and organic content) produced by our isolates, and (iii) evaluate the potential influence of the stalks on the mobility of metal cations, such as nickel in these habitats.

RESULTS

Isolation, phylogeny, and physiology of microaerophilic Fe(II) oxidizers. After 4 to 5 transfers in a dilution-to-extinction series on zero-valent iron (ZVI) pates, cell morphology appeared homogenous in fluorescence microscopy. Both cultures produced characteristic twisted stalks, which were easily recognizable via light microscopy (Fig. 2). The increase in numbers of cells and stalks observed microscopically after inoculation of ZVI plates, as well as the fact that since their isolation, the cultures have been successfully transferred >50 times under microaerophilic Fe(II)-oxidizing conditions on ZVI plates in the absence of any organic carbon or significant concentration of another inorganic electron donor, clearly demonstrated that the isolated strains are Fe(II) oxidizers.

Growth tests revealed that growth occurred only with Fe(II) provided as FeS in gradient tubes or as ZVI under microoxic conditions in plates, but not with any of the tested single substrates nor with complex media (Table 1). The cultures were considered to be pure, as no growth was found on any other substrate or complex media. Although the cultures could not grow on H_2 alone under microoxic conditions, we cannot, however, exclude that the growth on ZVI plates was partly promoted by the H_2 that is produced by reaction of the ZVI with H_2O. The isolates' ability to grow in FeS gradient tubes, where no H_2 is supplied, shows that H_2 is not required for growth.

The twisted stalks that formed during growth with FeS in gradient tubes were shorter and appeared to be less tightly coiled (Fig. 2) than those produced during growth on ZVI plates. Salinity tests showed that no growth occurred at salinities between 1.6 and 3.4, while between salinities of 6.9 and 23, normal cell growth with the presence of cells and twisted stalks were observed (Table 2). At a salinity of 5.2, only weak growth was observed, and compared to normal growth conditions, only a few

TABLE 1 Combinations of electron acceptors and electron donors on which growth of the two isolated strains of *Zetaproteobacteria* was tested[a]

Electron acceptor	Electron donor	Growth	Stalks
O_2[b]	FeS	+	+
O_2[b]	ZVI	+	+
O_2[b]	H_2	−	−
O_2[b]	$MnCl_2$	−	−
O_2[b]	S^0	−	−
O_2[b]	H_2SO_3	−	−
O_2[b]	DMSO	−	−
O_2[b]	H_2S	−	−
O_2[b]	Various organic substrates	−	−
O_2[c]	Various organic substrates	−	−
O_2[c]	LB or R2A (solid and liquid)	−	−
NO_3^-	Lactate/acetate/yeast extract	−	−
Fe(III)	Lactate/acetate/yeast extract	−	−
SO_4^{2-}	Lactate/acetate/yeast extract	−	−

[a]Both strains were able to grow with Fe(II) and O_2 only under microoxic conditions.
[b]Microoxic conditions.
[c]Full atmospheric oxygen concentration.

cells and twisted stalks were present. For the two isolated cultures, the same salinity dependence was observed. The decreasing salinity in our experiments represents a gradual transition from saltwater to freshwater conditions. Therefore, concentration changes of a particular medium component, e.g., magnesium, might have also affected bacterial growth. However, the complete absence of growth between salinities of 1.6 and 3.4 with all medium components still being present, even though at lower concentration, suggests that salinity is the main selective factor.

Phylogenetic analysis based on the 16S rRNA gene revealed that both isolates belong to the class *Zetaproteobacteria*. Both cultures were 94% identical to *Mariprofundus ferrooxydans* PV-1 (Fig. 3), indicating that they might belong to a genus other than *Mariprofundus*, which is currently the only genus within the *Mariprofundaceae*. However, to make a clear decision as to whether the isolates belong to a novel genus, the sequences obtained in this study are too short, and a more detailed genetic study is required to elucidate this.

Morphology of cells and twisted stalks. Microscopic analysis showed that cells of both Fe(II)-oxidizing strains were slightly curved rods approximately 1 μm long and 0.4 μm wide (Fig. 2F). Furthermore, it was found that for cells of both isolates, in cultures grown for a few days to a week on ZVI plates, most of the cells were associated with the network of twisted stalk filaments, and only a few cells were not attached to twisted stalks and were motile, probably by flagellar movement. In contrast, in older cultures (grown for $>$1 week), the number of cells being detached from twisted stalks and moving probably by flagellar movement was higher. The twisted stalks of both cultures were easily visible by light microscopy (Fig. 2). The culture from Norsminde Fjord produced stalks that were more finely structured than those produced by the Kalø Vig isolate (Fig. 2 and 4). In both cultures, but to a larger extent in the culture from Kalø Vig, the twisted stalks were aggregating, resulting in large patches of twisted stalk structures (Fig. 2A). The stalk surface was initially smooth, with some attached round aggregates (diameter, ~0.3 μm). In the Norsminde cultures, but to a greater extent in

TABLE 2 Salinity dependence of the growth of two strains of *Zetaproteobacteria* isolated from Norsminde Fjord and Kalø Vig[a]

Salinity	Growth	Stalks
1.6–3.4	−	−
5.2	+ (weak)	+ (few)
6.9–23	+	+

[a]The salinity dependence was determined with ZVI plates as the Fe(II) source, and the results shown are valid for both strains.

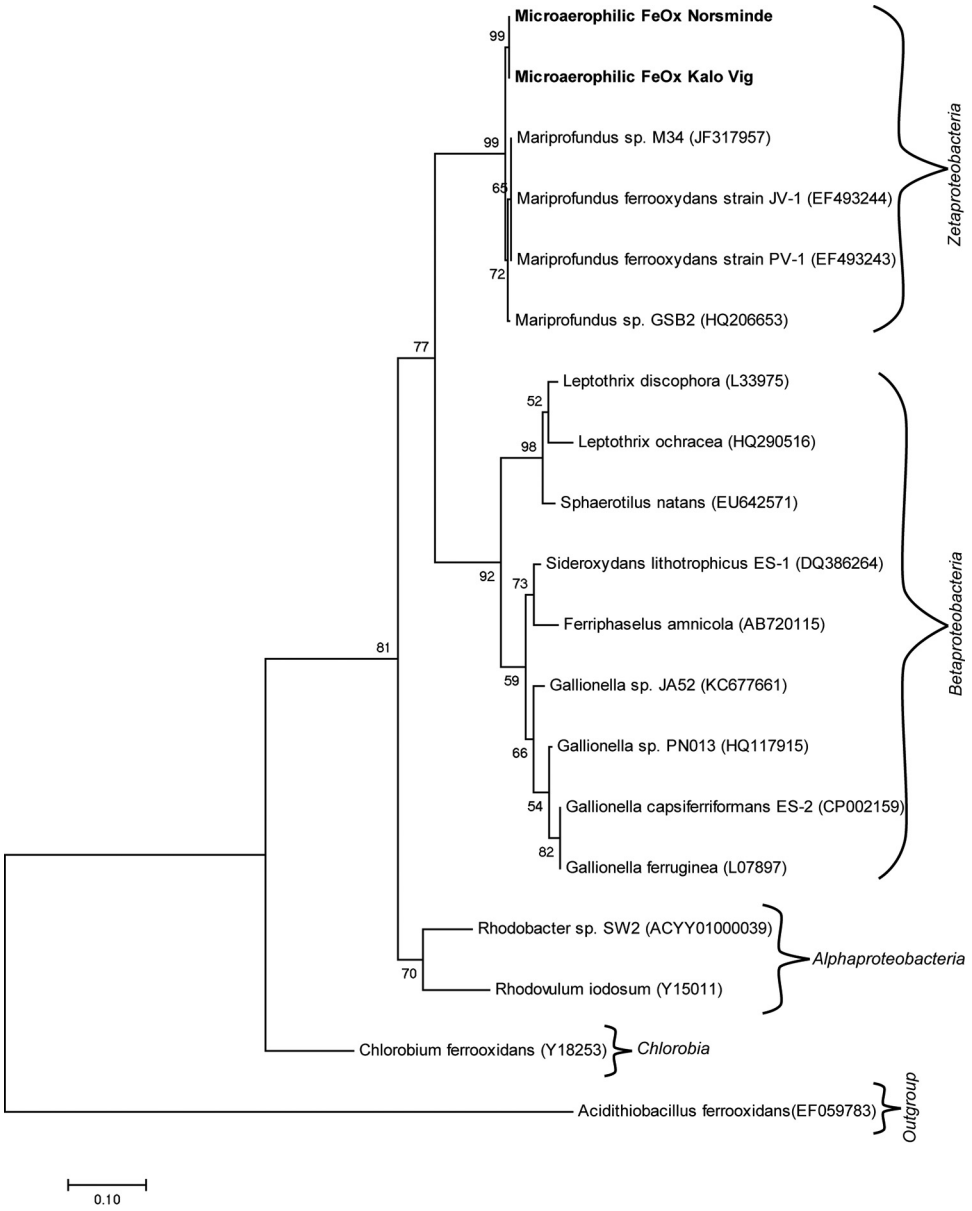

FIG 3 Phylogenetic tree constructed using the maximum likelihood method showing relationship based on the 16S rRNA gene between the two newly isolated *Zetaproteobacteria* from Norsminde and Kalø Vig and representative microaerophilic Fe(II) oxidizers and anoxygenic phototrophic Fe(II) oxidizers. The scale bar corresponds to 0.1 nucleotide substitutions per site. At the branches, bootstrap values (from 1,000 replications) are indicated. Accession numbers are shown in parentheses next to the organism names.

Kalø Vig cultures, the smooth stalk surface gradually became rough with clearly visible mineral spikes when grown for more than a few days on ZVI plates (Fig. 4). This change is possibly due to transformation of the initially poorly crystalline mineral precipitates to the more crystalline mineral phase lepidocrocite, which has also been observed by Chan et al. (29) on the surface of stalks produced by pure cultures of *Mariprofundus ferrooxydans* PV-1. It could also be clearly seen how multiple cell divisions lead to multiple branching of the twisted stalks (Fig. 2B). The length of the twisted stalks ranged from 15 to 78 μm in both cultures. Stalk width was evaluated by scanning electron microscopy analysis and ranged from 0.7 to 1 μm in the culture from Norsminde Fjord and from 1 to 1.5 μm in the culture from Kalø Vig (Fig. 4). The twisted stalks consisted of bundles of fibrils aligned parallel to the length of the stalk. The diameters of individual fibrils were ~0.15 μm in the culture from Norsminde Fjord and

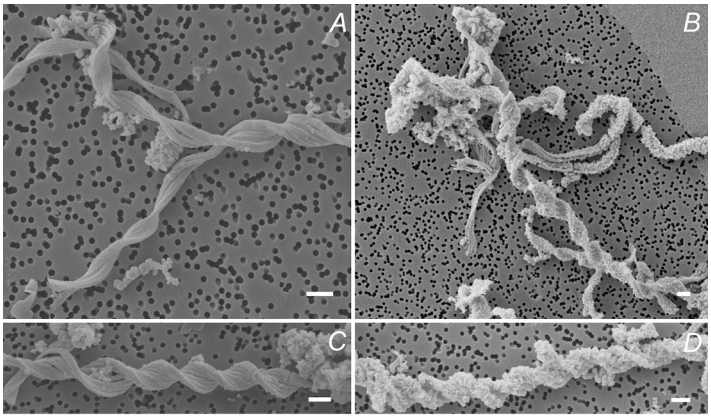

FIG 4 Scanning electron microscopy images of the microaerophilic Fe(II) oxidizers isolated from Norsminde Fjord (A and B) and Kalø Vig (C and D) grown on ZVI plates for 5 days. (A and C) Shown are mostly smooth stalk surfaces. (B and D) Shown are the spikey features that appear on the surface of some stalks when incubation time exceeds 4 days. Scale bars = 1 μm.

~0.2 μm in the culture from Kalø Vig. The stalks formed in the culture from Kalø Vig were generally more tightly coiled.

Stalk composition. X-ray diffraction analysis (μXRD) of Fe minerals in the twisted stalks showed signals for lepidocrocite (FeOOH) and halite in both cultures (Fig. 5). The halite observed in μXRD samples stems from the saltwater medium used for cultivation, which was not completely removed prior to drying of the samples. Mössbauer spectra

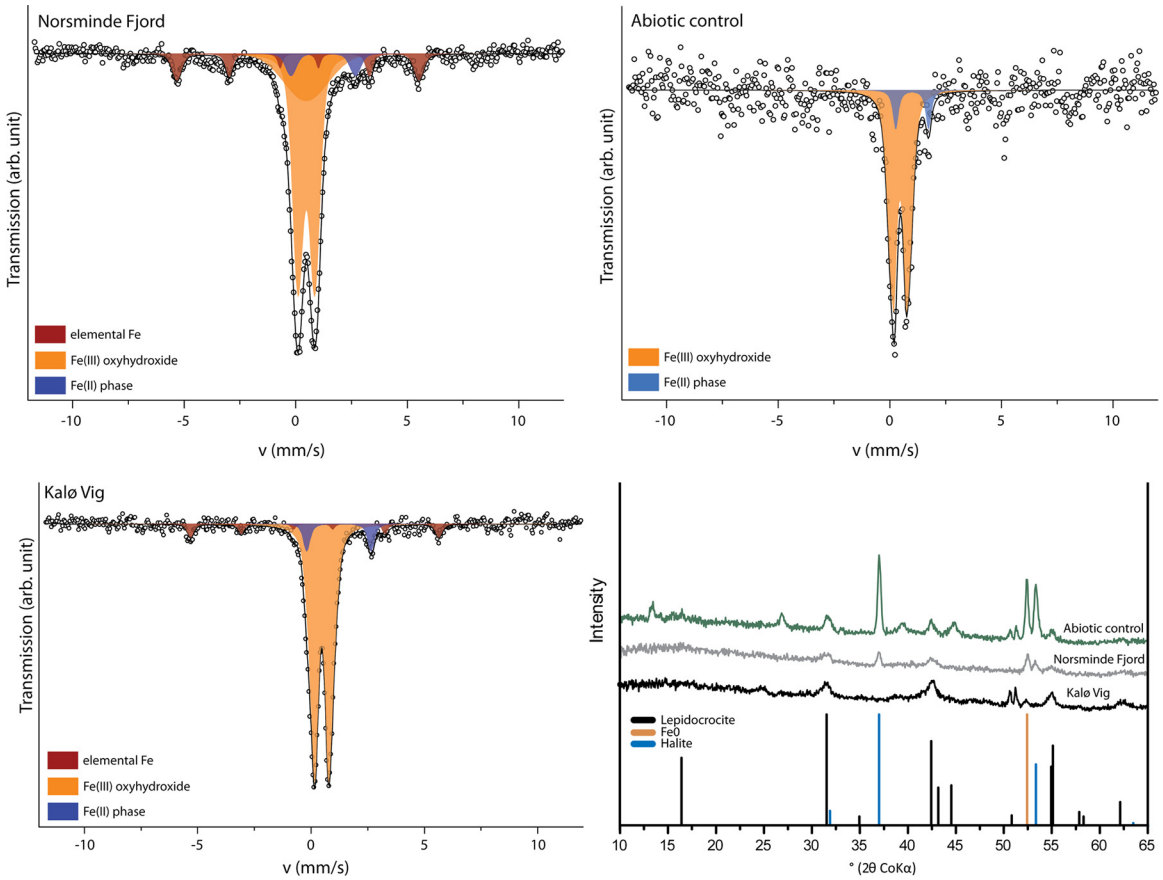

FIG 5 Mössbauer spectra collected at 77 K and μ-X-ray diffractograms (bottom right) of the Fe minerals formed in cultures of the microaerophilic Fe(II) oxidizers isolated from Norsminde Fjord, Kalø Vig, and abiotic controls. arb., arbitrary; v, velocity.

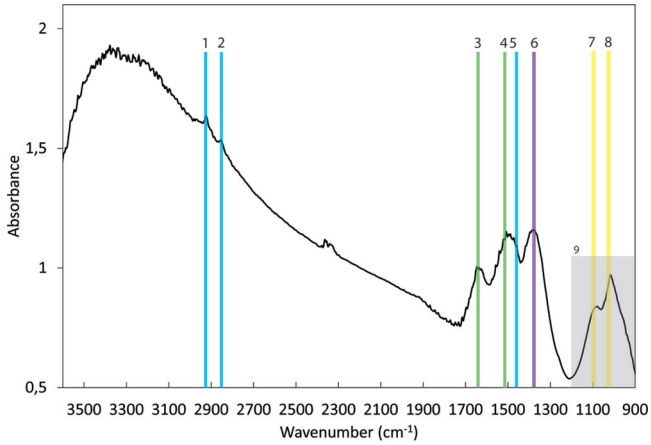

FIG 6 FTIR absorption measurements in focal plane array (FPA) mode performed on bulk samples containing twisted stalks formed by cultures from both Norsminde Fjord and Kalø Vig and small amounts of abiotically formed minerals: Bands 1, 2, and 5 (2,920, 2,850, and 1,460 cm^{-1}, respectively) are indicative of polymethylene chains found in most lipids which contain CH_2 groups. Band 3 (1,630 cm^{-1}) is consistent with the amide II absorption but could also be caused by molecular water that was not completely removed by freeze-drying. Band 4 (1,504 cm^{-1}) is indicative of the presence of the amino acid tryptophan and together with the amide II band suggests the presence of a small amount of protein. Membrane lipids possibly account for band 6 (1,368 cm^{-1}). Bands 7 and 8 (1,100 and 1,020 cm^{-1}, respectively) have been suggested to correspond to ionized -P-O- and -P-OH, respectively, and overlap those of lepidocrocite. Absorption in the range of 800 to 1,200 cm^{-1} (9) corresponds to the fingerprint region of polysaccharides. However, the low intensity of bands in this region does not allow an unambiguous assignment to polysaccharides. The band doublet at 2,350 and 2,330 cm^{-1} is due to molecular CO_2 accumulation in the atmosphere during the measurement. Bands were assigned using references 46 and 47.

revealed the presence of elemental Fe [Fe(0)], an Fe(II) phase, and at least one Fe(III) phase. The Fe(III) component of the Mössbauer spectra showed characteristics for Fe(III) oxyhydroxides with magnetic splitting below 77 K, as for lepidocrocite (45). However, the presence of ferrihydrite is also possible, because it shows Mössbauer absorption properties at 77 K very similar to those of lepidocrocite, so that the two Mössbauer absorption patterns cannot be distinguished. Due to its poor crystallinity, ferrihydrite is not easily identified by μXRD. The small amounts of 8 mol% and 6 mol% Fe(II) (of total Fe) as well as the 8 mol% and 11 mol% Fe(0) (of total Fe) detected in the Kalø Vig and Norsminde Fjord isolates, respectively, probably stem from the Fe source in the growth medium and might be deposited on the stalk surface during filtration in sample preparation. We quantified the carbon and nitrogen content of the stalks in pooled samples from both cultures to evaluate the amount of organic material present in the stalk structure and found ~0.3 wt% carbon and 0.04 wt% nitrogen. To further characterize the organic components in the stalks, we used Fourier transform infrared (FTIR) spectroscopy (Fig. 6), as well as on pooled samples from both cultures. The spectrum was assigned using references 46–48. The presence of absorption bands at 2,920 cm^{-1} and 2,850 cm^{-1} (Fig. 6, bands 1 and 2) is indicative of polymethylene chains found in most lipids, which contain CH_2 groups. -CH and -CH_2 asymmetric stretching (out of plane) generates an absorption band at 2,926 cm^{-1}, and the -CH_2 symmetric stretching (in plane) produces a band at 2,853 cm^{-1}. -CH_2 bends or scissors vibrations would also contribute an absorption band at 1,460 cm^{-1} (Fig. 6, band 5). The lack of well-defined peaks above 3,000 cm^{-1} suggests the absence of =C-H groups and the presence of mostly saturated aliphatic chains. However, the broad absorption feature in this region of the spectrum with the maximum at ~3,500 cm^{-1} is associated with the fundamental -OH stretch vibration of water. Weak bands at 920 and 970 cm^{-1} may arise from $N^+(CH_3)_3$ symmetric and antisymmetric stretches in lipids. A -CH_3 antisymmetric bend can generate an absorption band, potentially explaining the observed band at 1,460 cm^{-1} (Fig. 6, band 5). Membrane lipids possibly account for the band at 1,368 cm^{-1} (Fig. 6, band 6). The band at 1,630 cm^{-1} (Fig. 6, band 3) is consistent with the amide

II absorption band, but the bending mode of molecular H_2O would also create a band at 1,640 cm^{-1}. Therefore, in case H_2O was not completely removed by freeze-drying, it could also cause or contribute to this band. The absorption band at 1,504 cm^{-1} (Fig. 6, band 4) could be explained by aromatic -C=C- and indicates the presence of the amino acid tryptophan (Trp), with a -C=C absorption reported at 1,622 cm^{-1}, and a C-N stretching vibration combined with an N-H bending absorption at 1,509 cm^{-1}, also corresponding to the amide II arrangement. This is an indication for a small portion of protein present in the stalk structure. The bands observed at 1,020 and 1,100 cm^{-1} (Fig. 6, bands 7 and 8) have been suggested to correspond to ionized -P-O- and -P-OH, respectively. However, lepidocrocite also generates characteristic bands at 1,018 and 1,161 cm^{-1}. Absorption in the range of 800 to 1,200 cm^{-1} (Fig. 6, region 9) corresponds to the fingerprint region of polysaccharides. However, based on the FTIR data alone, an unambiguous assignment to polysaccharides is not possible. To confirm the presence of polysaccharides, we also analyzed the stalks by confocal laser scanning microscopy (CLSM). Stalks of both strains bound the lectins wheat germ agglutinin (WGA) and peanut agglutinin (PGA), indicating the presence of polysaccharides (Fig. 7). Binding of WGA was weaker than PNA in cultures from Norsminde Fjord, while stalks from cultures from Kalø Vig bound less PNA than WGA. Binding also varies within stalks and between different stalks from the same culture, indicating a heterogeneous polysaccharide content of the stalks. Consistent with the FTIR results, we found poor binding of the protein stain NanoOrange in both cultures (Fig. 7).

Immobilization of Ni by twisted stalks. We used time of flight-secondary ion mass spectrometry (TOF-SIMS) to analyze to which extent the stalks formed by the Fe(II)-oxidizing culture from Norsminde Fjord immobilize and bind the trace metal ion Ni^{2+}. The stalks' area is well defined by the distribution of Fe (indicated by the Fe^+ ion yield) and revealed a heterogeneous distribution of Ni^{2+} (measured as the Ni^+ ion yield) throughout the stalks' structure (Fig. 8). There are a few spots in the stalks' area which show an increased Ni^+ ion yield. These spots could be due to higher Ni^{2+} concentrations indicating Ni^{2+} precipitates or areas with high Ni^{2+} sorption capacity. However, it has to be kept in mind that small fluctuations in Ni^+ ion yields could to some extent also be caused by a heterogeneous composition within the stalks' area affecting the ion yield due to matrix effects. Therefore, the presented maps of Ni^{2+} distribution are to be considered qualitative data. This is due to the heterogeneous composition of the stalks, which meant it was not possible to measure suitable Ni^{2+}-containing organo-mineral reference compounds, thus preventing a more accurate quantitative analysis of the Ni^{2+} content.

DISCUSSION

Diversity and geographic distribution of *Zetaproteobacteria* in marine systems. Previous studies in coastal marine habitats have provided evidence for the presence of *Zetaproteobacteria* in coastal waters off Maine, USA, and China, where they were detected on submerged metal-Fe surfaces, as well as in low-Fe sediments of the Skagerrak (17, 18, 49) and in estuarine Fe-rich mats (50). Here, we present further indications that *Zetaproteobacteria* are not restricted to habitats with elevated Fe concentrations but also seem to be widespread in typical coastal marine sediments that contain lower Fe concentrations. These findings and evidence from molecular data (Fig. 1) indicate that microaerophilic Fe(II) oxidizers belonging to the *Zetaproteobacteria* group (potentially) have a higher geographical distribution than previously thought. The adaptation to a broad salinity range observed for our isolates supports this broad geographical distribution. As shown by McAllister et al. (20), *Zetaproteobacteria* are diverse and exhibit a biogeographic pattern, with 16S rRNA sequences differing more between samples that originate from more distant sampling sites (also found by Scott et al. [21]). However, so far, sequences mostly from Fe-rich habitats were compared, and it is not known how similar or different these sequences are compared to *Zetaproteobacteria* from low-Fe habitats. Our isolates that stem from low-Fe sedimentary habitats in Aarhus, Denmark, increase the diversity of available zetaproteobacterial cultures, in

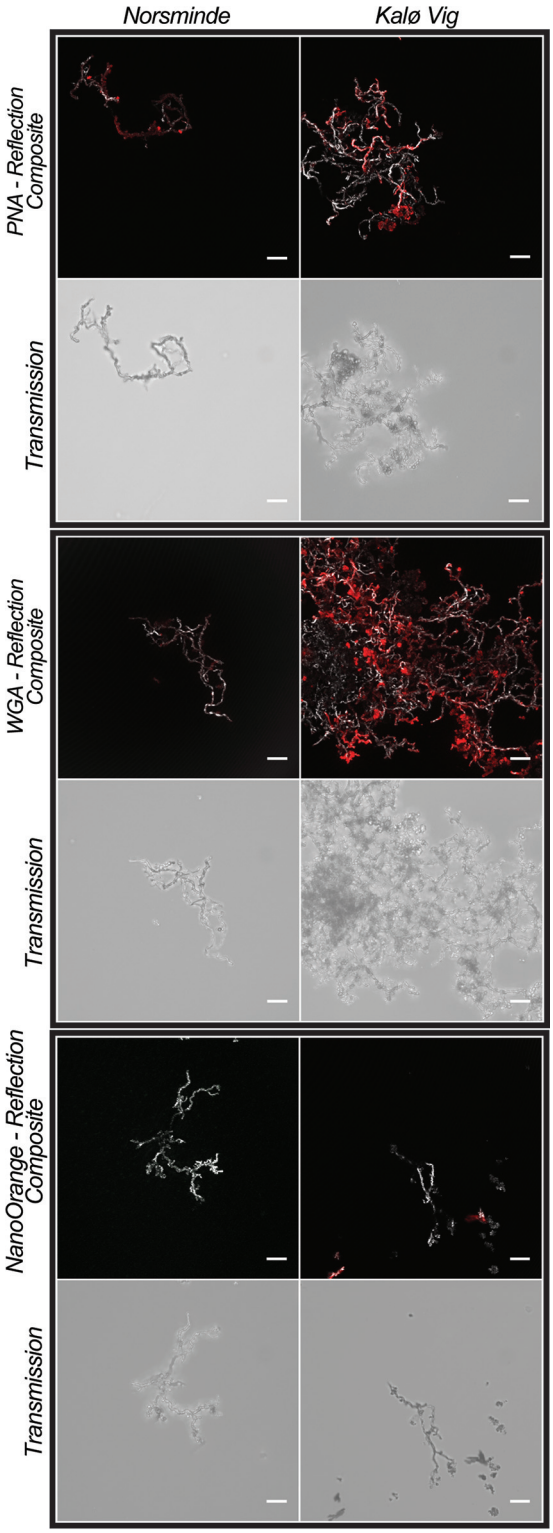

FIG 7 Confocal laser scanning microscopy images of stalks of the two microaerophilic Fe(II) oxidizers that were isolated from Norsminde and Kalø Vig stained with three fluorescent dyes: PNA-Alexa Fluor conjugate (peanut agglutinin, specific for terminal β-galactose residues), WGA-Alexa Fluor conjugate (wheat germ agglutinin, specific for *N*-acetylglucosamine and *N*-acetylneuraminic acid), and NanoOrange (specific for proteins). In colored composite images, the stalks are visualized in gray by their reflection signal of the laser, and fluorescence stain signals are presented in red. For each sample, an additional nonconfocal transmitted light image of the stalks is shown. In composite images of samples stained with NanoOrange, the histogram was stretched linearly to a saturation of 0.3% of the pixels for better visibility of the stalks' reflection. Scale bars = 10 μm.

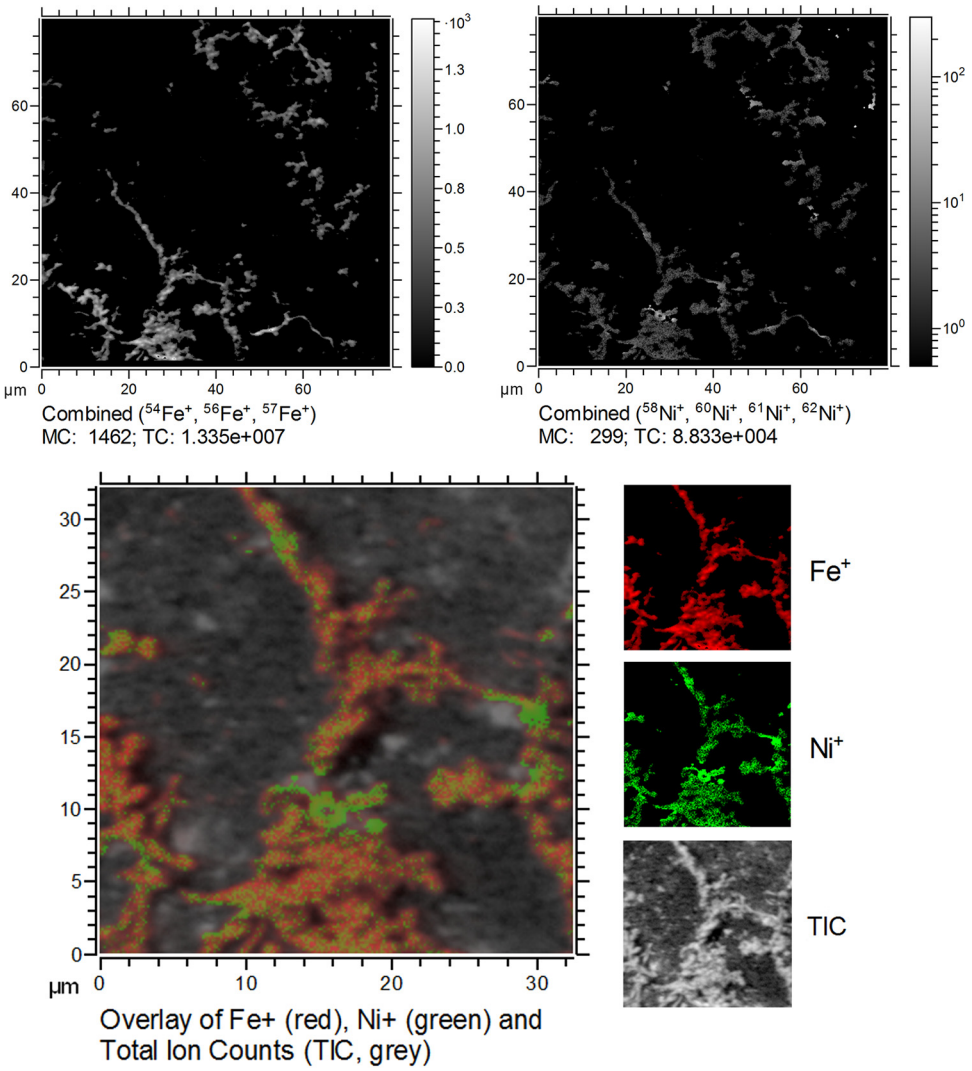

FIG 8 TOF-SIMS measurements of stalks produced by the isolates from Norsminde Fjord grown on ZVI plates in artificial seawater medium containing 100 nM Ni^{2+}. The upper images show the distribution of Ni^+ and Fe^+ ion yield (mind the different intensity scaling) within the area of the twisted stalks (defined by the Fe^+ ion yield map). The lower image shows an overlay of both ion yield maps (Fe^+ in red, Ni^+ in green). MC, mass counts (in pixels); TIC, total ion counts.

particular since they have only 94% sequence identity to *Mariprofundus ferrooxydans* PV-1. All other isolates are 96 to 99% identical to each other. It can also be seen in the phylogenetic tree (Fig. 3) that our two isolates from Aarhus cluster together and are distinct from the other isolates. This shows that the two isolated *Zetaproteobacteria* from low-Fe habitats are (based on 16S rRNA gene analysis) different from those isolated from high-Fe habitats. However, since the small number of isolated *Zetaproteobacteria* does not reflect the diversity of *Zetaproteobacteria* found in both types of environments, a comparison of further sequences is necessary to establish whether *Zetaproteobacteria* from low-Fe environments generally differ from those found in high-Fe habitats.

In comparison to Scott et al. (21), who reported "little evidence for *Zetaproteobacteria* in marine environments outside of iron-rich systems," where "iron-rich" in this study was defined by a high content of Fe (oxyhydr)oxides, we have demonstrated that these microorganisms are present in coastal low-Fe sediments from Norsminde Fjord and Kalø Vig. Such typical marine sediments are usually found at the coasts or at continental shelfs, which comprise about 7% of the total area of the world's oceans (51).

Therefore, this significantly increases the known habitats of *Zetaproteobacteria*, which were previously thought to be mainly Fe-rich systems, e.g., systems influenced by hydrothermal venting. As a consequence, *Zetaproteobacteria* could contribute a much larger portion to global Fe cycling than previously thought.

Physiology of *Zetaproteobacteria* isolated from low-Fe coastal marine sediments. The microaerophilic Fe(II)-oxidizing isolates from Norsminde Fjord and Kalø Vig were only 94% identical to other isolated *Zetaproteobacteria* on the basis of 16S rRNA gene identity. However, like the other isolated *Zetaproteobacteria*, they only grew autotrophically by Fe(II) oxidation under microoxic conditions and not via oxidation of several tested organic substrates. H_2, which is formed on the ZVI plates used for cultivation during Fe(0) corrosion, was not used alone for autotrophic growth but could potentially supplement the Fe-based metabolism. These findings suggest that our strains are obligate chemolithoautotrophs. This means that they could only be active in a very restricted area in the sediment due to the shallow oxygen penetration in these coastal sediments. Therefore, one ensuing question is: what would be the benefit of being an obligate microaerophilic Fe(II) oxidizer in this low-Fe habitat? This question was also raised previously for other obligate photo- and chemolithoautotrophic sulfur-oxidizing microorganisms (52). However, so far, there is no fully satisfactory answer to this question (52). It is believed that obligate chemolithoautotrophs have some advantages compared to facultative chemolithoautotrophs, e.g., the specialization by having a higher substrate affinity than facultative chemolithoautotrophs, as observed for some aerobic sulfur oxidizers (53–55). However, the disadvantage is that they are dependent on the occurrence of specific environmental conditions in order to be active and oxidize iron(II). To some extent, *Zetaproteobacteria* seem to be adapted to changing environmental conditions, such that they can at least survive when geochemical conditions are changing. The genetic potential for aerotaxis and production of antioxidants has been found, as well as the potential for energy storage in the form of organic carbon (56). Recently, it has also been shown that *Zetaproteobacteria* are able to store energy in the form of polyphosphates (56, 57). The authors postulated that the polyphosphates are produced by *Zetaproteobacteria* using ATP in times when they can perform Fe(II) oxidation and can be used to produce energy to survive under conditions where they cannot gain energy from Fe(II) oxidation (57). It remains to be determined if the uncultivated *Zetaproteobacteria* that are present in the natural habitats are also obligate chemolithoautotrophs or if the currently applied isolation techniques are selective for this type (23). The potential for mixotrophy was found in a sequenced genome of an isolate (58). Additionally, in sequenced genomes of uncultivated *Zetaproteobacteria*, the potential for mixotrophy or even heterotrophy, as well as the potential for other chemolithoautotrophic metabolisms (e.g., sulfide oxidation), were found (23, 58).

Microbial Fe cycling involving microaerophilic Fe(II)-oxidizing *Zetaproteobacteria*. In a previous study, it was shown that Fe(III)-reducing bacteria are present and coexist with microaerophilic Fe(II) oxidizers within the same layers in sediment from Norsminde Fjord and Kalø Vig (25). As shown by Roden and coworkers (59) using cocultures of a lithoautotrophic microaerophilic Fe(II) oxidizer and an anaerobic dissimilatory Fe(III) reducer, grown in a column system that provided an oxygen gradient, there is the potential for microscale Fe cycling in such stratified systems. The potential for Fe cycling and the coexistence of Fe(III) reducers and Fe(II) oxidizers was also demonstrated in deep-sea Fe-rich systems (60). However, deep-sea systems are often limited in organic carbon, which decreases the potential for Fe cycling in these systems, as the activity of heterotrophic dissimilatory Fe(III) reducers is limited by the availability of their electron donor (60). In organic-rich coastal sediments, such as those from Norsminde Fjord studied here, there is potential for more active Fe cycling between microaerophilic Fe(II) oxidizers and Fe(III) reducers, because (i) the higher organic carbon content of these coastal sediments would favor the activity of heterotrophic dissimilatory Fe(III)-reducing bacteria and (ii) daily and seasonal fluctuations in the oxygen penetration depth would allow for temporally separated Fe cycling between

microaerophilic Fe(II) oxidizers and anaerobic Fe(III) reducers in the oxic-anoxic transition zone. Therefore, the presence of autotrophic Fe(II)-oxidizing *Zetaproteobacteria*, which produce Fe(III) minerals that can serve as electron acceptors for heterotrophic Fe(III) reducers, in low-Fe sediments also increases their potential contribution to Fe cycling, because of the favorable conditions for Fe(III) reduction in these habitats.

Potential physiological role of twisted stalk formation. Both isolated microaerophilic Fe(II)-oxidizing *Zetaproteobacteria* presented in this study produced the characteristic twisted stalks that have been observed in other isolated *Zetaproteobacteria* (17, 22, 29) and many microaerophilic Fe(II) oxidizers from freshwater habitats (reviewed in reference 7). As suggested by Krepski et al. (33), the production of twisted stalks by bacteria from such different habitats and their occurrence in all isolated *Zetaproteobacteria* indicate an important physiological role of these structures for microaerophilic Fe oxidation. According to the model proposed by Chan et al. (29), they enable the bacteria to direct precipitation of the Fe(III) oxyhydroxides away from the cell, which, along with a neutral-charge hydrophilic cell surface (61), prevents cell encrustation (29, 62).

We observed that the shapes of the stalks in our cultures were different depending on the growth conditions. Fewer and shorter stalks were formed in cultures that were grown in gradient tubes than in cultures that were grown in ZVI plates. A likely explanation for this observation is the different concentrations and gradients of O_2 and Fe(II) that are present in gradient tubes and ZVI plates. While in the ZVI plates O_2 concentrations over time are relatively stable, in the gradient tubes, the gradients of O_2 and Fe(II) are changing over time [due to consumption of O_2 and changes in Fe(II) release from the bottom Fe(II) source] so that in the gradient tubes, it is likely that the cells have to move in order to react to these changes and follow the optimum growth conditions. In order to move, the cells have to either detach from the twisted stalks, which could explain the shorter twisted stalks that were seen in the gradient tubes than in the ZVI plates, or the cells have to direct the stalk growth toward optimal conditions along the oxygen gradient.

Mineral formation and transformation at the twisted stalks. Mössbauer spectroscopy and μXRD showed the presence of lepidocrocite in the stalks. However, the existence of an additional ferrihydrite phase is possible. The occurrence of lepidocrocite has also been observed by Chan et al. (29) on the surface of stalks mainly consisting of ferrihydrite produced by pure cultures of *Mariprofundus ferrooxydans* PV-1. Formation of lepidocrocite is likely in systems with high salinity, particularly in the presence of chloride (46). We therefore assume that stalks formed by our bacteria initially contain ferrihydrite that transforms into lepidocrocite on the surface of the stalk over time. This is consistent with the observed changes from a smooth stalk surface to the occurrence of spike-like features on the surface with increasing incubation time. These spike-like features are similar to the blade-like structures observed by Chan et al. (29). Since both studies were conducted with pure cultures, transformation of ferrihydrite could be faster in these experiments than observed in environmental samples (31) due to less adsorption of silica and organic material, which slows down mineral transformation (31). This would be consistent with the absence of silica from the growth medium and the low organic carbon fraction we found in our stalks.

Organic compounds in the twisted stalks. We found a low fraction of organic carbon (ca. 0.3 wt%) in the stalks by total organic carbon (TOC) measurements. However, these results are only an estimation, because it is not possible to fully avoid the presence of remaining zero-valent Fe particles during sampling. Even though the actual organic carbon content therefore could be slightly higher, it would still be fairly low. In the organic carbon fraction of the twisted stalks, we found polysaccharides, saturated aliphatic compounds (most probably lipids), and a very small amount of protein. Similar compounds have been detected in stalks of other marine and also freshwater microaerophilic Fe(II)-oxidizing bacteria, but not all authors detected lipids (29, 32–35). The indication of membrane lipids we found by FTIR could be due to the

adsorption of cellular material, which might also be true for the detected protein. Nevertheless, the organic compounds identified in stalks produced by microaerophilic Fe(II)-oxidizing bacteria seem to be consistent based on spectroscopic analyses used for their identification. This suggests that the mechanism of stalk production is similar among microaerophilic bacteria. We tried to determine which specific organic compounds are present in the stalks using matrix-assisted laser desorption ionization–time of flight (MALDI-TOF) mass spectrometry, but measurements were not successful, probably due to the low organic content in the stalks. It has to be noted that during the necessary washing steps with double-distilled water in FTIR and TOC sample preparation, the remaining cells in the sample potentially released organic material due to osmotic shock. These released organic molecules are expected to adsorb to the stalks, as described by Bennett et al. (35). However, most cells were removed from the samples before washing with double-distilled water in previous separation steps of cells and stalks with artificial seawater (ASW).

Twisted stalks as a sink for Ni^{2+}. Our study clearly showed that stalks formed by the Fe(II)-oxidizing isolate from Norsminde Fjord immobilize the trace metal ion Ni^{2+}. Even though we could assess Ni^{2+} immobilization by the stalks only qualitatively because of the lack of an appropriate reference compound due to the heterogeneity of the sample, our TOF-SIMS results are in general agreement with previous findings by Schmid et al. (34). They demonstrated Ni^{2+} immobilization for stalks produced by microaerophilic Fe(II)-oxidizing bacteria collected from an abandoned mine. Sorption of other transition metals to twisted stalks has also been reported (31, 34, 35, 37, 63). Therefore, the presence of twisted stalks affects the availability of transition metals not only for the stalk-forming bacteria but also for other microorganisms. Sorption of transition metals to the stalks will increase their local concentration on the stalk surface while initially decreasing their concentration in the surrounding aqueous phase. If transformation to more crystalline iron mineral phases with a lower surface area occurs at the stalk's surface, transition metals will be released again to the surrounding aqueous phase. In marine habitats, localized sorption of nickel to twisted stalks may have a high impact. For example, at the Lō'ihi Seamounts (24), dense mats of Fe minerals formed by microaerophilic Fe(II)-oxidizing bacteria are present and potentially scavenge transition metals exported from these vents, which has been reported for other hydrothermal vent systems (64). Furthermore, Fe mats formed by microaerophilic Fe(II)-oxidizing bacteria found on continental margin sediments (12) may impact the transition of organic compounds and transition metals from the water column into the sediment. Since *Zetaproteobacteria* are only present at low numbers (25) in the sediments in Aarhus Bay, the formation of dense mats of twisted stalks seems unlikely, and therefore, an effect of stalks formed by these bacteria on Ni^{2+} availability is probably restricted to microniches. However, considering the wide distribution of *Zetaproteobacteria* (17, 21, 22, 25, 50), their impact on trace metal availability might be higher in other marine habitats. In ancient ocean environments, Fe(II) was abundant, oxygen was present at microoxic concentrations, and nickel concentrations were much higher (65–67) than in modern marine habitats (~9 nM [68]). Thus, the sequestration of nickel by twisted stalks formed by microaerophilic Fe(II)-oxidizing bacteria may have played an important role. Microaerophilic Fe(II)-oxidizing bacteria are also common members of microbial communities at plant roots in terrestrial habitats (69), and sorption of nickel and other metals to Fe minerals formed by these bacteria will affect their availability for the rest of the microbial root community and the plants.

Conclusions and outlook. By isolating microaerophilic Fe(II)-oxidizing *Zetaproteobacteria* from typical low-Fe coastal marine sediments, we increased the knowledge regarding their geographical distribution and their contribution to the biogeochemical Fe cycle. Furthermore, we showed that isolates from low-Fe sediments share the characteristic properties of the *Zetaproteobacteria* group, regarding their physiology and stalk composition, with isolates originating from habitats with high Fe concentrations. We could also show that stalks produced by *Zetaproteobacteria* potentially

influence the availability of metal cations, such as nickel, for other microorganisms. The methods applied for isolation of the novel strains of *Zetaproteobacteria* from low-Fe environments presented here were similar to methods that were previously applied for the isolation of microaerophilic Fe(II)-oxidizing bacteria from high-Fe environments (17, 20, 22, 24). As shown by Field et al. (23), slight changes in the methods that are used for isolation can lead to isolates with different physiological characteristics. To better assess the physiological and phylogenetic diversity of *Zetaproteobacteria*, further isolation attempts should be made with inoculation material originating from environments with distinctly different geochemical characteristics. Moreover, other isolation strategies, e.g., using different Fe sources and concentrations, varying the oxygen content, varying pressure, or providing an organic cosubstrate, should be tested. This all would help further increase knowledge about the geographical distribution and physiological properties of *Zetaproteobacteria* and confirm or disprove the obligate chemolithoautotrophic nature of this bacterial group.

MATERIALS AND METHODS

Isolation and cultivation. Microaerophilic Fe(II) oxidizers were isolated and cultivated in zero-valent iron (ZVI) plates with artificial seawater (ASW) medium and CO_2 as a carbon source, as described by Laufer et al. (25). Briefly, ZVI plates are petri dishes containing ZVI powder and ASW, incubated under microoxic conditions (O_2 = 6 to 10% of atmospheric O_2), that are created with gas packs (BD GasPak EZ Campy; Becton, Dickinson and Co., NJ) inside anoxic jars (Merck, Darmstadt, Germany). Both Fe(II)-oxidizing isolates originate from coastal sediments (water depth, <1 m) located in Aarhus Bay, Denmark. The first field site, Norsminde Fjord (56°1.171′N, 10°15.390′E), is a shallow estuary with a narrow opening to the Baltic Sea. The sediment is muddy and organic rich. Salinity at this field site varied between 14 and 23 and depended on local wind and local precipitation. The second field site at Kalø Vig (56°16.81′N, 10°28.056′E) is a sandy beach, where the sediment has a low organic carbon content. Salinity at this field site varied between 20 and 23. The applied isolation strategy supplied bacteria with low O_2 concentrations (6 to 10% atmospheric O_2 concentration) and low Fe^{2+} concentrations (50 to 300 μM [22]) and thus should mimic well the environmental conditions under which they are expected to live in sediments at the two field sites. Culture growth was checked regularly by fluorescence microscopy and a LIVE/DEAD BacLight bacterial viability kit (Molecular Probes, Carlsbad, CA, USA).

Physiological characterization of the isolates. For physiological characterization of the isolates, we tested combinations of different electron acceptors [O_2, NO_3^-, SO_4^{2-}, and Fe(III)] and electron donors [different organic substrates, Fe(II) (ZVI and FeS), H_2S, S^0, $S_2O_3^{2-}$, Mn(IV), dimethyl sulfoxide (DMSO), and H_2], as listed in Table 1. The following organic substrates were tested under both atmospheric oxygen concentrations and with ca. 10% atmospheric oxygen concentrations: yeast extract (2 g/liter) and acetate, lactate, propionate, fumarate, succinate, butyrate, formate, pyruvate, citrate, benzoate, ethanol, cysteine, glutamate, glucose, saccharose, glycerol, mannitol, and peptone (all 4 mM concentration). Furthermore, the growth under atmospheric oxygen concentrations on the following complex growth media were tested: LB-ASW and R2A-ASW agar plates and liquid LB-ASW medium. Growth under anoxic conditions with the electron acceptors NO_3^-, SO_4^{2-}, and Fe(III) (4 mM each) was tested in Hungate tubes containing 9 ml of ASW medium, 1 ml of a culture that was grown on ZVI plates, and either acetate, lactate, or yeast extract (same concentrations described above). Growth under microoxic conditions on inorganic substrates was tested either on ZVI plates (only for ZVI and S^0), in gel-stabilized gradient tubes [for FeS, H_2S, S^0, $S_2O_3^{2-}$, Mn(IV), and DMSO], or in Hungate tubes (15 ml) containing 9 ml of ASW and 1 ml of the culture and a headspace of H_2/CO_2 (80/20), to which 0.5 ml of sterile air was added. The gradient tubes consisted of a top layer of ASW that contained 0.15% agarose and a bottom layer that consisted of ASW and 1.5% agarose. To the bottom layer, the different inorganic substrates were added at concentrations from 2 to 10 mM. The gradient tubes were prepared completely anoxic and closed with butyl stoppers until inoculation. For inoculation, the gradient tubes were opened under oxic and sterile conditions, and 100 μl of a culture that was grown on ZVI plates was inoculated to the top layer. To ensure that the headspace of the gradient tubes contained enough oxygen, they were left opened for 1 min after inoculation and were afterwards closed with butyl stoppers again. The growth was investigated visually, based on turbidity or color changes in the different setups and by fluorescence microscopy and LIVE/DEAD staining. All tests were done in duplicate.

For testing salinity dependence, we used different mixing ratios of the ASW medium and a freshwater medium (modified Wolfe's mineral medium [MWMM]). The MWMM contained, per liter, 0.1 g of NH_4Cl, 0.2 g of $MgSO_4 \cdot 7H_2O$, 0.1 g of $CaCl_2 \cdot 2H_2O$, and 0.05 g of K_2HPO_4. The buffer and the pH were the same as for the ASW. The MWMM had a salinity of 1.6 (measured with a multimeter [Multi 3430; WTW] equipped with a conductivity electrode [TetraCon92; WTW]). The salinity range tested was consequently 1.6 (only MWMM) to 23 (only ASW), and 12 different salinity levels were tested in duplicate. The tests were done on ZVI plates. Growth was investigated by fluorescence microscopy and LIVE/DEAD staining.

Phylogenetic characterization. Phylogenetic analysis of the isolates and construction of the phylogenetic tree, including related autotrophic Fe(II)-oxidizing bacteria, were conducted based on the 16S rRNA gene. DNA from cultures of both isolates (grown on ZVI plates) was extracted with the UltraClean microbial DNA isolation kit (Mo Bio Laboratories, Inc., Carlsbad, CA, USA), according to the instructions

of the manufacturer. A PCR to obtain 16S rRNA gene fragments was performed with the general bacterial 16S rRNA gene-specific primers GM3-F (5′-AGAGTTTGATCMTGGCTCAG-3′) (70) and 1392-R (5′-ACGGGC GGTGTGTRC-3′) (71). The resulting PCR products were loaded on a 1% agarose gel, and the bands were excised and cleaned with the Wizard PCR cleanup system (Promega Laboratories, WI). The cleaned-up DNA was cloned using the Qiagen PCR cloning kit (Qiagen, Germany). The plasmid vectors were transformed into competent cells (*Escherichia coli* DH5α) and plated onto LB medium containing ampicillin, isopropyl-β-D-thiogalactopyranoside (IPTG), and 5-bromo-4-chloro-3-indolyl-β-D-galactopyranoside (X-Gal) for blue/white screening. White colonies were picked and tested for their correct insert size. Overnight cultures were prepared from colonies with the correct inserts in 5 ml of liquid LB medium containing ampicillin. Plasmid DNA was isolated from these cultures and sent to GATC Biotech (Constance, Germany) for sequencing. For each isolate, at least three clones were picked and sequenced. The quality testing of the resulting sequences and trimming of the sequences were performed with the software Geneious R6 (Biomatters). The sequences were then assigned to bacterial phyla using the online Ribosomal Database Project (RDP) naive Bayesian classifier version 2.2 (http://rdp.cme.msu.edu/classifier/classifier.jsp).

For constructing a phylogenetic tree, the 16S rRNA gene sequences from closely related, as well as more distantly related, autotrophic Fe(II)-oxidizing bacteria (microaerophilic and anoxygenic phototrophic Fe(II) oxidizers) were downloaded from the EMBL database. Bacterial 16S rRNA gene sequences from two species belonging to different phyla than the Fe(II) oxidizer sequences were chosen as outgroups. ClustalW (72) was used for alignment of the 16S rRNA gene sequences. Phylogenetic trees were constructed by the maximum likelihood method with the software package MEGA7 (73).

Transmission light, fluorescence, confocal laser scanning, and electron microscopic analyses. Transmission light and fluorescence microscopy were performed with a Leica DM5500 B epifluorescence microscope equipped with a 40× air objective (numerical aperture, 0.75) and a 100× oil immersion objective (numerical aperture, 1.4). The filter sets applied were L5 (excitation filter, band-pass [BP] 480/40 nm; dichromatic mirror, 505 nm; suppressor filter, BP 527/39) and Y3 (excitation filter, BP 543/30; dichromatic mirror, 565 nm; suppressor filter, BP 610/75). Cells were stained with the LIVE/DEAD BacLight bacterial viability kit (Molecular Probes, Carlsbad, CA, USA). Confocal laser scanning microscopy (CLSM) was performed on a Leica SPE confocal laser scanning microscope equipped with an ACS APO 63× water immersion objective (numerical aperture, 1.15). Polysaccharides were stained with a PNA-Alexa Fluor 647 conjugate (Molecular Probes; 8.58 μg/ml final concentration) and a WGA-Alexa Fluor 647 conjugate (Molecular Probes; 8.58 μg/ml final concentration). Proteins were stained with NanoOrange (0.5 μl/6.5 μl sample; Molecular Probes). Staining was performed on individual samples for each dye. Samples were rinsed with ASW medium after staining. The PNA-Alexa Fluor 647 and the WGA-Alexa Fluor 647 conjugates were excited with a 635-nm laser and emission recorded between 647 nm and 780 nm and 650 and 720 nm, respectively (on individual samples). NanoOrange was excited at 488 nm and emission recorded between 560 and 680 nm. Samples for scanning electron microscopy (SEM) were prepared similarly to those by Krepski et al. (33). Briefly, 50 μl of sample was taken from ZVI plates, diluted in 5 ml of sterile water, filtered onto 0.2-μm-pore-size GTTP polycarbonate filters (Isopore, Merck, Darmstadt, Germany), and air dried. Filters were coated with 8 nm of Pt using a Bal-Tec SCD 005 sputter coater (Balzers, Liechtenstein) and examined in a LEO 1450 VP SEM (Zeiss, Oberkochen, Germany) at 5 kV acceleration voltage and 5 mm working distance using an Everhart-Thornley secondary electron detector.

Mineralogical analysis by Mössbauer spectroscopy and μXRD. For Mössbauer spectroscopy, the mineral precipitates were recovered on a 0.45-μm-pore-size syringe filter that was embedded between Kapton tape foils. The sample was inserted into a closed-cycle exchange gas cryostat (SHI-650-5; Janis Research, Woburn, MA, USA). The spectra were recorded at 77 K in transmission geometry using a constant-acceleration drive system (WissEl, Starnberg, Germany). A ^{57}Co source embedded in a rhodium matrix was used as gamma radiation source. The sample spectra were calibrated against a 7-μm-thick α-[^{57}Fe] foil at room temperature (RT). The RECOIL software suite (University of Ottawa, Canada) was used for the calibration and the modeling of the spectra. The spectra were modeled using Voigt-based line shapes. The Lorentz half-width-half-maximum (HWHM) value was kept constant at the minimum line width of the 3 and 4 peaks of the calibration foil (0.124 mm/s and 0.129 mm/s, respectively) in the models, and the Gauss' sigma parameter was used to account for line broadening until the fitting was reasonable. The sample spectra were analyzed with respect to the center shift (CS) values, the quadrupole splitting (Δ), and hyperfine fields (H). ZVI plates that have not been inoculated with bacteria and incubated for the same time as the bacterial samples were used as abiotic controls.

Samples for μXRD were dried and ground in an anoxic glove box (100% N_2), deposited on a silicon wafer, and stored in N_2-filled jars until analysis under air (within a few minutes to avoid oxidation of O_2-sensitive Fe minerals). A Bruker D8 Discover GADDS XRD^2-microdiffractometer (Bruker Optik, Ettlingen, Germany) was used, equipped with a Co anode, a primary graphite monochromator, and a 2-dimensional Hi-Star detector. Minerals were identified using the internal database of the EVA software (version 10.0.1.0).

Elemental analysis and FTIR. For total organic carbon (TOC), nitrogen content, and Fourier transform infrared (FTIR) spectroscopy measurements of the twisted stalks that contained Fe minerals and organic carbon, samples containing mixtures of stalks and bacteria were transferred from ZVI plates to Falcon tubes, omitting the bottom layer of zero-valent Fe. Cells were separated from the stalks by shaking the Falcon tubes gently by hand. The Fe-containing stalks were allowed to sediment, and the supernatant containing most cells was removed. This step was repeated two times with ASW medium, and the absence of most cells in the stalk fraction was confirmed by fluorescence microscopy. The stalks

were then washed twice with sterile double-distilled water to remove salts and freeze-dried in a Christ Alpha 1-4 LD freeze-dryer (Christ, Osterode, Germany). For TOC measurements, 12 mg of stalk material was dissolved in 50 μl of 36% HCl. The acid was allowed to evaporate in a fume hood overnight. TOC and nitrogen content were measured with a CN element analyzer (vario EL; Elementar, Hanau, Germany). FTIR measurements of the stalks were performed on a Bruker Vertex 80V (Bruker Optik GmbH, Ettlingen, Germany), using a Globar light source and a KBr beamsplitter. Absorption spectra were collected from 3,950 to 950 cm^{-1} at a spectral resolution of 4 cm^{-1}. FTIR measurements were performed with a focal plane array (FPA) detector (64 by 64 elements; pixel size, 2.7 by 2.7 μm; field of view, 170 by 170 μm) attached to the Hyperion 3000 microscope (15× Cassegrain objective) on freeze-dried stalk material deposited on a 1-mm-thick single crystal calcium fluoride window. The spectra were collected with 1,024 scans (averaged) in transmission mode. Reference measurements were performed on a calcium fluoride window without sample.

TOF-SIMS. Nickel immobilization by twisted stalks was analyzed by time of flight-secondary ion mass spectrometry (TOF-SIMS). Cells were grown on ZVI plates with ASW medium containing 100 nM Ni^{2+} that was also used in all other experiments. Samples from the Norsminde Fjord isolate were filtered onto polycarbonate filters precoated with Au/Pd, as described for SEM samples, using acid-washed equipment (1 M HCl) whenever possible. Measurements were performed with a TOF-SIMS.5 (ION-TOF GmbH, Muenster, Germany) in positive extraction mode employing 30 keV Bi^+ primary ion beam from a NanoProbe LMIG source delivering 0.05 pA of primary Bi^+ ions in 100-ns pulses with a 70-μs repetition period over a 80 by 80 μm^2 sample area in 512 by 512 pixel raster. The used imaging mode of TOF-SIMS.5 operation in combination with delayed extraction has provided a lateral resolution of about 130 nm and mass resolving power (MRP) above 3,000. The analysis was performed in 437 scans/planes with 10 shots of Bi^+ primary ions per pixel rastered randomly over the analysis area. The acquired scans were accumulated after shift correction, and the resulting total stack was analyzed for lateral distribution of ion yield using SurfaceLab 6.5 software (ION-TOF GmbH, Muenster, Germany).

Accession number(s). Good-quality sequences were uploaded to the EMBL/GenBank database (accession numbers LT575232 and LT575233).

ACKNOWLEDGMENTS

We thank Wiebke Ruschmeier for help with preparing gradient tubes, Karin Stögerer for help with molecular biological analyses, Ellen Struve for TOC measurements, Annette Flicker for help with the FTIR measurements, and Hartmut Schulz for help with electron microscopy analysis and for freeze-drying the stalk samples. Furthermore, we want to thank Aude Picard for helpful discussions about the composition of the twisted stalks. We acknowledge the Centre for Chemical Microscopy (ProVIS) at the Helmholtz Centre for Environmental Research supported by European Regional Development Funds (EFRE–Europe funds Saxony) for using their analytical facilities for TOF-SIMS analysis.

The European Research Council (ERC) provided funding to K. Laufer, M. Nordhoff, and A. Kappler under grant 307320-MICROFOX.

REFERENCES

1. Ehrenberg GC. 1836. Vorlaufige Mitteilungen über das wirkliche Vorkommen Fossiler Infusorien und ihre grosse Verbreitung. Poggendorff Ann 38:213–227.
2. Lieske R. 1911. Beiträge zur Kenntnis der Physiologie von Spirophyllum ferrugineum Ellis, einem typischen Eisenbakterium. Jahrb Wiss Bot 49:91–99.
3. Davison W, Seed G. 1983. The kinetics of the oxidation of ferrous iron in synthetic and natural waters. Geochim Cosmochim Acta 47:67–79. https://doi.org/10.1016/0016-7037(83)90091-1.
4. Millero FJ, Sotolongo S, Izaguirre M. 1987. The oxidation kinetics of Fe(II) in seawater. Geochim Cosmochim Acta 51:793–801. https://doi.org/10.1016/0016-7037(87)90093-7.
5. Druschel GK, Emerson D, Sutka R, Suchecki P, Luther GW, III. 2008. Low-oxygen and chemical kinetic constraints on the geochemical niche of neutrophilic iron(II) oxidizing microorganisms. Geochim Cosmochim Acta 72:3358–3370. https://doi.org/10.1016/j.gca.2008.04.035.
6. Rentz JA, Kraiya C, Luther GW, III, Emerson D. 2007. Control of ferrous iron oxidation within circumneutral microbial iron mats by cellular activity and autocatalysis. Environ Sci Technol 41:6084–6089. https://doi.org/10.1021/es062203e.
7. Emerson D, Fleming EJ, McBeth JM. 2010. Iron-oxidizing bacteria: an environmental and genomic perspective. Annu Rev Microbiol 64:561–583. https://doi.org/10.1146/annurev.micro.112408.134208.
8. Sobolev D, Roden EE. 2004. Characterization of a neutrophilic, chemolithoautotrophic Fe(II)-oxidizing beta-proteobacterium from freshwater wetland sediments. Geomicrobiol J 21:1–10. https://doi.org/10.1080/01490450490253310.
9. Emerson D, Moyer C. 1997. Isolation and characterization of novel iron-oxidizing bacteria that grow at circumneutral pH. Appl Environ Microbiol 63:4784–4792.
10. Hegler F, Lösekann-Behrens T, Hanselmann K, Behrens S, Kappler A. 2012. Influence of seasonal and geochemical changes on the geomicrobiology of an iron carbonate mineral water spring. Appl Environ Microbiol 78:7185–7196. https://doi.org/10.1128/AEM.01440-12.
11. Kato S, Krepski S, Chan C, Itoh T, Ohkuma M. 2014. Ferriphaselus amnicola gen. nov., sp. nov., a neutrophilic, stalk-forming, iron-oxidizing bacterium isolated from an iron-rich groundwater seep. Int J Syst Evol Microbiol 64:921–925. https://doi.org/10.1099/ijs.0.058487-0.
12. Rubin-Blum M, Antler G, Tsadok R, Shemesh E, Austin JA, Jr, Coleman DF, Goodman-Tchernov BN, Ben-Avraham Z, Tchernov D. 2014. First evidence for the presence of iron-oxidizing Zetaproteobacteria at the Levantine continental margins. PLoS One 9:e91456. https://doi.org/10.1371/journal.pone.0091456.
13. Edwards KJ, Rogers DR, Wirsen CO, McCollom TM. 2003. Isolation and characterization of novel psychrophilic, neutrophilic, Fe-oxidizing, chemolithoautotrophic alpha- and gamma-proteobacteria from the deep sea. Appl Environ Microbiol 69:2906–2913. https://doi.org/10.1128/AEM.69.5.2906-2913.2003.
14. Edwards KJ, Glazer BT, Rouxel OJ, Bach W, Emerson D, Davis RE, Toner BM, Chan CS, Tebo BM, Staudigel H, Moyer CL. 2011. Ultra-diffuse

hydrothermal venting supports Fe-oxidizing bacteria and massive umber deposition at 5000 m off Hawaii. ISME J 5:1748–1758. https://doi.org/10.1038/ismej.2011.48.
15. Forget NL, Murdock SA, Juniper SK. 2010. Bacterial diversity in Fe-rich hydrothermal sediments at two South Tonga Arc submarine volcanoes. Geobiology 8:417–432. https://doi.org/10.1111/j.1472-4669.2010.00247.x.
16. Kato S, Kobayashi C, Kakegawa T, Yamagishi A. 2009. Microbial communities in iron-silica-rich microbial mats at deep-sea hydrothermal fields of the Southern Mariana Trough. Environ Microbiol 11:2094–2111. https://doi.org/10.1111/j.1462-2920.2009.01930.x.
17. McBeth JM, Little BJ, Ray RI, Farrar KM, Emerson D. 2011. Neutrophilic iron-oxidizing "Zetaproteobacteria" and mild steel corrosion in nearshore marine environments. Appl Environ Microbiol 77:1405–1412. https://doi.org/10.1128/AEM.02095-10.
18. Dang H, Chen R, Wang L, Shao S, Dai L, Ye Y, Guo L, Huang G, Klotz MG. 2011. Molecular characterization of putative biocorroding microbiota with a novel niche detection of Epsilon- and Zetaproteobacteria in Pacific Ocean coastal seawaters. Environ Microbiol 13:3059–3074. https://doi.org/10.1111/j.1462-2920.2011.02583.x.
19. Field EK, Kato S, Findlay AJ, MacDonald DJ, Chiu BK, Luther GW, Chan CS. 2016. Planktonic marine iron oxidizers drive iron mineralization under low-oxygen conditions. Geobiology 14:499–508. https://doi.org/10.1111/gbi.12189.
20. McAllister SM, Davis RE, McBeth JM, Tebo BM, Emerson D, Moyer CL. 2011. Biodiversity and emerging biogeography of the neutrophilic iron-oxidizing zetaproteobacteria. Appl Environ Microbiol 77:5445–5457. https://doi.org/10.1128/AEM.00533-11.
21. Scott JJ, Breier JA, Luther GW, III, Emerson D. 2015. Microbial iron mats at the Mid-Atlantic Ridge and evidence that Zetaproteobacteria may be restricted to iron-oxidizing marine systems. PLoS One 10:e0119284. https://doi.org/10.1371/journal.pone.0119284.
22. Emerson D, Rentz JA, Lilburn TG, Davis RE, Aldrich H, Chan C, Moyer CL. 2007. A novel lineage of proteobacteria involved in formation of marine Fe-oxidizing microbial mat communities. PLoS One 2:e667. https://doi.org/10.1371/journal.pone.0000667.
23. Field EK, Sczyrba A, Lyman AE, Harris CC, Woyke T, Stepanauskas R, Emerson D. 2014. Genomic insights into the uncultivated marine Zetaproteobacteria at Loihi Seamount. ISME J 9:857–870.
24. Emerson D, Moyer CL. 2002. Neutrophilic Fe-oxidizing bacteria are abundant at the Loihi Seamount hydrothermal vents and play a major role in Fe oxide deposition. Appl Environ Microbiol 68:3085–3093. https://doi.org/10.1128/AEM.68.6.3085-3093.2002.
25. Laufer K, Nordhoff M, Røy H, Schmidt C, Behrens S, Jørgensen BB, Kappler A. 2016. Coexistence of microaerophilic, nitrate-reducing, and phototrophic Fe(II) oxidizers and Fe(III) reducers in coastal marine sediment. Appl Environ Microbiol 82:1433–1447. https://doi.org/10.1128/AEM.03527-15.
26. Thamdrup B, Fossing H, Jørgensen BB. 1994. Manganese, iron and sulfur cycling in a coastal marine sediment, Aarhus bay, Denmark. Geochim Cosmochim Acta 58:5115–5129. https://doi.org/10.1016/0016-7037(94)90298-4.
27. Neubauer SC, Emerson D, Megonigal JP. 2002. Life at the energetic edge: kinetics of circumneutral iron oxidation by lithotrophic iron-oxidizing bacteria isolated from the wetland-plant rhizosphere. Appl Environ Microbiol 68:3988–3995. https://doi.org/10.1128/AEM.68.8.3988-3995.2002.
28. Emerson D. 2000. Microbial oxidation of Fe(II) and Mn(II) at circumneutral pH, p 31–52. *In* Lovley DR (ed), Environmental microbe-metal interactions. ASM Press, Washington, DC.
29. Chan CS, Fakra SC, Emerson D, Fleming EJ, Edwards KJ. 2011. Lithotrophic iron-oxidizing bacteria produce organic stalks to control mineral growth: implications for biosignature formation. ISME J 5:717–727. https://doi.org/10.1038/ismej.2010.173.
30. Fleming EJ, Davis RE, McAllister SM, Chan CS, Moyer CL, Tebo BM, Emerson D. 2013. Hidden in plain sight: discovery of sheath-forming, iron-oxidizing Zetaproteobacteria at Loihi Seamount, Hawaii, USA. FEMS Microbiol Ecol 85:116–127. https://doi.org/10.1111/1574-6941.12104.
31. Toner BM, Berquo TS, Michel FM, Sorensen JV, Templeton AS, Edwards KJ. 2012. Mineralogy of iron microbial mats from Loihi Seamount. Front Microbiol 3:118.
32. Picard A, Kappler A, Schmid G, Quaroni L, Obst M. 2015. Experimental diagenesis of organo-mineral structures formed by microaerophilic Fe(II)-oxidizing bacteria. Nat Commun 6:6277. https://doi.org/10.1038/ncomms7277.
33. Krepski ST, Hanson TE, Chan CS. 2012. Isolation and characterization of a novel biomineral stalk-forming iron-oxidizing bacterium from a circumneutral groundwater seep. Environ Microbiol 14:1671–1680. https://doi.org/10.1111/j.1462-2920.2011.02652.x.
34. Schmid G, Zeitvogel F, Hao L, Ingino P, Adaktylou I, Eickhoff M, Obst M. 2016. Submicron-scale heterogeneities in nickel sorption of various cell-mineral aggregates formed by Fe(II)-oxidizing bacteria. Environ Sci Technol 50:114–125. https://doi.org/10.1021/acs.est.5b02955.
35. Bennett S, Toner B, Barco R, Edwards K. 2014. Carbon adsorption onto Fe oxyhydroxide stalks produced by a lithotrophic iron-oxidizing bacteria. Geobiology 12:146–156. https://doi.org/10.1111/gbi.12074.
36. Barco RA, Edwards KJ. 2014. Interactions of proteins with biogenic iron oxyhydroxides and a new culturing technique to increase biomass yields of neutrophilic, iron-oxidizing bacteria. Front Microbiol 5:259.
37. Chan CS, Fakra SC, Edwards DC, Emerson D, Banfield JF. 2009. Iron oxyhydroxide mineralization on microbial extracellular polysaccharides. Geochim Cosmochim Acta 73:3807–3818. https://doi.org/10.1016/j.gca.2009.02.036.
38. Hohmann C, Morin G, Ona-Nguema G, Guigner J-M, Brown GE, Jr, Kappler A. 2011. Molecular-level modes of As binding to Fe(III) (oxyhydr) oxides precipitated by the anaerobic nitrate-reducing Fe(II)-oxidizing Acidovorax sp. strain BoFeN1. Geochim Cosmochim Acta 75:4699–4712. https://doi.org/10.1016/j.gca.2011.02.044.
39. Eickhoff M, Obst M, Schröder C, Hitchcock AP, Tyliszczak T, Martinez RE, Robbins LJ, Konhauser KO, Kappler A. 2014. Nickel partitioning in biogenic and abiogenic ferrihydrite: the influence of silica and implications for ancient environments. Geochim Cosmochim Acta 140:65–79. https://doi.org/10.1016/j.gca.2014.05.021.
40. Martinez RE, Pedersen K, Ferris FG. 2004. Cadmium complexation by bacteriogenic iron oxides from a subterranean environment. J Colloid Interface Sci 275:82–89. https://doi.org/10.1016/j.jcis.2004.02.018.
41. Martinez RE, Smith DS, Pedersen K, Ferris FG. 2003. Surface chemical heterogeneity of bacteriogenic iron oxides from a subterranean environment. Environ Sci Technol 37:5671–5677. https://doi.org/10.1021/es0342603.
42. Konhauser KO, Kappler A, Roden EE. 2011. Iron in microbial metabolisms. Elements 7:89–93. https://doi.org/10.2113/gselements.7.2.89.
43. Mulrooney SB, Hausinger RP. 2003. Nickel uptake and utilization by microorganisms. FEMS Microbiol Rev 27:239–261. https://doi.org/10.1016/S0168-6445(03)00042-1.
44. Kennedy C, Scott S, Ferris F. 2003. Characterization of bacteriogenic iron oxide deposits from Axial Volcano, Juan de Fuca Ridge, northeast Pacific Ocean. Geomicrobiol J 20:199–214. https://doi.org/10.1080/01490450303873.
45. Murad E, Cashion J. 2004. Iron oxides, p 159–188. *In* Murad E, Cashion J (ed), Mössbauer spectroscopy of environmental materials and their industrial utilization. Springer Science+Business Media, New York, NY.
46. Cornell R, Schwertmann U. 2003. The iron oxides: structure, properties, reactions, occurences [*sic*] and uses. Wiley-VCH Verlag GmbH, Weinheim, Germany.
47. Barth A. 2000. The infrared absorption of amino acid side chains. Prog Biophys Mol Biol 74:141–173. https://doi.org/10.1016/S0079-6107(00)00021-3.
48. Tamm LK, Tatulian SA. 1997. Infrared spectroscopy of proteins and peptides in lipid bilayers. Q Rev Biophys 30:365–429. https://doi.org/10.1017/S0033583597003375.
49. Reyes C, Dellwig O, Dähnke K, Gehre M, Noriega-Ortega B, Böttcher ME, Meister P, Friedrich MW. 2016. Bacterial communities potentially involved in iron-cycling in Baltic Sea and North Sea sediments revealed by pyrosequencing. FEMS Microbiol Ecol 92:fiw054. https://doi.org/10.1093/femsec/fiw054.
50. McBeth JM, Fleming EJ, Emerson D. 2013. The transition from freshwater to marine iron-oxidizing bacterial lineages along a salinity gradient on the Sheepscot River, Maine, USA. Environ Microbiol Rep 5:453–463. https://doi.org/10.1111/1758-2229.12033.
51. Yool A, Fasham MJ. 2001. An examination of the "continental shelf pump" in an open ocean general circulation model. Glob Biogeochem Cycles 15:831–844. https://doi.org/10.1029/2000GB001359.
52. Wood AP, Aurikko JP, Kelly DP. 2004. A challenge for 21st century molecular biology and biochemistry: what are the causes of obligate autotrophy and methanotrophy? FEMS Microbiol Rev 28:335–352. https://doi.org/10.1016/j.femsre.2003.12.001.

53. Smith A, Kelly D. 1979. Competition in the chemostat between an obligately and a facultatively chemolithotrophic Thiobacillus. J Gen Microbiol 115:377–384. https://doi.org/10.1099/00221287-115-2-377.
54. Kuenen J, Robertson L, Tuovienen O. 1992. The genera Thiobacillus, Thiomicrospira and Thiosphaera, p 2638–2657. *In* Balows A, Truper HG, Dworkin M, Harder W, Schleifer K-H (ed), The prokaryotes, 2nd ed, vol III. Springer, New York, NY.
55. Kuenen J, Beudeker R. 1982. Microbiology of thiobacilli and other sulphur-oxidizing autotrophs, mixotrophs and heterotrophs. Philos Trans R Soc Lond B Biol Sci 298:473–497. https://doi.org/10.1098/rstb.1982.0093.
56. Singer E, Emerson D, Webb EA, Barco RA, Kuenen JG, Nelson WC, Chan CS, Comolli LR, Ferriera S, Johnson J, Heidelberg JF, Edwards KJ. 2011. Mariprofundus ferrooxydans PV-1 the first genome of a marine Fe(II) oxidizing zetaproteobacterium. PLoS One 6:e25386. https://doi.org/10.1371/journal.pone.0025386.
57. Hoshino T, Kuratomi T, Morono Y, Hori T, Oiwane H, Kiyokawa S, Inagaki F. 2016. Ecophysiology of Zetaproteobacteria associated with shallow hydrothermal iron-oxyhydroxide deposits in Nagahama Bay of Satsuma Iwo-Jima, Japan. Front Microbiol 6:1554.
58. Singer E, Heidelberg JF, Dhillon A, Edwards KJ. 2013. Metagenomic insights into the dominant Fe(II) oxidizing Zetaproteobacteria from an iron mat at Loi'hi, Hawai'i. Front Microbiol 4:52.
59. Roden EE, Sobolev D, Glazer B, Luther GW. 2004. Potential for microscale bacterial Fe redox cycling at the aerobic-anaerobic interface. Geomicrobiol J 21:379–391. https://doi.org/10.1080/01490450490485872.
60. Emerson D. 2009. Potential for iron-reduction and iron-cycling in iron oxyhydroxide-rich microbial mats at Loihi Seamount. Geomicrobiol J 26:639–647. https://doi.org/10.1080/01490450903269985.
61. Saini G, Chan CS. 2013. Near-neutral surface charge and hydrophilicity prevent mineral encrustation of Fe-oxidizing micro-organisms. Geobiology 11:191–200. https://doi.org/10.1111/gbi.12021.
62. Thamdrup B, Glud RN, Hansen JW. 1994. Manganese oxidation and *in situ* manganese fluxes from a coastal sediment. Geochim Cosmochim Acta 58:2563–2570. https://doi.org/10.1016/0016-7037(94)90032-9.
63. Suzuki T, Hashimoto H, Matsumoto N, Furutani M, Kunoh H, Takada J. 2011. Nanometer-scale visualization and structural analysis of the inorganic/organic hybrid structure of Gallionella ferruginea twisted stalks. Appl Environ Microbiol 77:2877–2881. https://doi.org/10.1128/AEM.02867-10.
64. Sander S, Koschinsky A. 2016. The export of iron and other trace metals from hydrothermal vents and the impact on their marine biogeochemical cycle, p 9–24. *In* Demina LL, Galkin SV (ed), The handbook of environmental chemistry, vol 50. Springer, New York, NY.
65. Anbar AD. 2008. Elements and evolution. Science 322:1481–1483. https://doi.org/10.1126/science.1163100.
66. Canfield DE. 2005. The early history of atmospheric oxygen: homage to Robert M. Garrels. Annu Rev Earth Planet Sci 33:1–36. https://doi.org/10.1146/annurev.earth.33.092203.122711.
67. Konhauser KO, Pecoits E, Lalonde SV, Papineau D, Nisbet EG, Barley ME, Arndt NT, Zahnle K, Kamber BS. 2009. Oceanic nickel depletion and a methanogen famine before the Great Oxidation Event. Nature 458:750–753. https://doi.org/10.1038/nature07858.
68. Drever JI. 1997. The geochemistry of natural waters: surface and groundwater environments. Prentice Hall, Upper Saddle River, NJ.
69. Weiss JV, Emerson D, Backer SM, Megonigal JP. 2003. Enumeration of Fe(II)-oxidizing and Fe(III)-reducing bacteria in the root zone of wetland plants: implications for a rhizosphere iron cycle. Biogeochemistry 64:77–96. https://doi.org/10.1023/A:1024953027726.
70. Muyzer G, Teske A, Wirsen CO, Jannasch HW. 1995. Phylogenetic relationships of Thiomicrospira species and their identification in deep-sea hydrothermal vent samples by denaturing gradient gel electrophoresis of 16S rDNA fragments. Arch Microbiol 164:165–172. https://doi.org/10.1007/BF02529967.
71. Lane DJ, Pace B, Olsen GJ, Stahl DA, Sogin ML, Pace NR. 1985. Rapid determination of 16S ribosomal RNA sequences for phylogenetic analyses. Proc Natl Acad Sci U S A 82:6955–6959. https://doi.org/10.1073/pnas.82.20.6955.
72. Thompson JD, Higgins DG, Gibson TJ. 1994. CLUSTAL W: improving the sensitivity of progressive multiple sequence alignment through sequence weighting, position-specific gap penalties and weight matrix choice. Nucleic Acids Res 22:4673–4680. https://doi.org/10.1093/nar/22.22.4673.
73. Kumar S, Stecher G, Tamura K. 2016. MEGA7: Molecular Evolutionary Genetics Analysis version 7.0 for bigger datasets. Mol Biol Evol 33:1870–1874. https://doi.org/10.1093/molbev/msw054.
74. Moyer CL, Dobbs FC, Karl DM. 1995. Phylogenetic diversity of the bacterial community from a microbial mat at an active, hydrothermal vent system, Loihi Seamount, Hawaii. Appl Environ Microbiol 61:1555–1562.
75. Rassa AC, McAllister SM, Safran SA, Moyer CL. 2009. Zeta-Proteobacteria dominate the colonization and formation of microbial mats in low-temperature hydrothermal vents at Loihi Seamount, Hawaii. Geomicrobiol J 26:623–638. https://doi.org/10.1080/01490450903263350.
76. Hodges TW, Olson JB. 2009. Molecular comparison of bacterial communities within iron-containing flocculent mats associated with submarine volcanoes along the Kermadec Arc. Appl Environ Microbiol 75:1650–1657. https://doi.org/10.1128/AEM.01835-08.
77. Kato S, Yanagawa K, Sunamura M, Takano Y, Ishibashi J, Kakegawa T, Utsumi M, Yamanaka T, Toki T, Noguchi T. 2009. Abundance of Zetaproteobacteria within crustal fluids in back-arc hydrothermal fields of the Southern Mariana Trough. Environ Microbiol 11:3210–3222. https://doi.org/10.1111/j.1462-2920.2009.02031.x.
78. Kato S, Ikehata K, Shibuya T, Urabe T, Ohkuma M, Yamagishi A. 2015. Potential for biogeochemical cycling of sulfur, iron and carbon within massive sulfide deposits below the seafloor. Environ Microbiol 17:1817–1835. https://doi.org/10.1111/1462-2920.12648.
79. Jan C, Petersen JM, Werner J, Teeling H, Huang S, Glöckner FO, Golyshina OV, Dubilier N, Golyshin PN, Jebbar M, Cambon-Bonavita M-A. 2014. The gill chamber epibiosis of deep-sea shrimp Rimicaris exoculata: an in-depth metagenomic investigation and discovery of Zetaproteobacteria. Environ Microbiol 16:2723–2738. https://doi.org/10.1111/1462-2920.12406.
80. Henri PA, Rommevaux-Jestin C, Lesongeur F, Mumford A, Emerson D, Godfroy A, Menez B. 2015. Structural iron(II) of basaltic glass as an energy source for Zetaproteobacteria in an abyssal plain environment, off the Mid Atlantic Ridge. Front Microbiol 6:1518.
81. Emerson JB, Thomas BC, Alvarez W, Banfield JF. 2015. Metagenomic analysis of a high CO_2 subsurface microbial community populated by chemolithoautotrophs and bacteria and archaea from candidate phyla. Environ Microbiol 18:1686–1703.
82. Ionescu D, Heim C, Polerecky L, Ramette A, Haeusler S, Bizic-Ionescu M, Thiel V, De Beer D. 2015. Diversity of iron oxidizing and reducing bacteria in flow reactors in the Äspö Hard Rock Laboratory. Geomicrobiol J 32:207–220. https://doi.org/10.1080/01490451.2014.884196.
83. Peng X, Ta K, Chen S, Zhang L, Xu H. 2015. Coexistence of Fe(II)- and Mn(II)-oxidizing bacteria govern the formation of deep sea umber deposits. Geochim Cosmochim Acta 169:200–216. https://doi.org/10.1016/j.gca.2015.09.011.
84. Crossey LJ, Karlstrom KE, Schmandt B, Crow RR, Colman DR, Cron B, Takacs-Vesbach CD, Dahm CN, Northup DE, Hilton DR, Ricketts JW, Lowry AR. 2016. Continental smokers couple mantle degassing and distinctive microbiology within continents. Earth Planet Sci Lett 435:22–30. https://doi.org/10.1016/j.epsl.2015.11.039.
85. Sylvan JB, Pyenson BC, Rouxel O, German CR, Edwards KJ. 2012. Time-series analysis of two hydrothermal plumes at 9°50′N East Pacific Rise reveals distinct, heterogeneous bacterial populations. Geobiology 10:178–192. https://doi.org/10.1111/j.1472-4669.2011.00315.x.
86. Eder W, Jahnke LL, Schmidt M, Huber R. 2001. Microbial diversity of the brine-seawater interface of the Kebrit Deep, Red Sea, studied via 16S rRNA gene sequences and cultivation methods. Appl Environ Microbiol 67:3077–3085. https://doi.org/10.1128/AEM.67.7.3077-3085.2001.
87. Sudek LA, Templeton AS, Tebo BM, Staudigel H. 2009. Microbial ecology of Fe (hydr)oxide mats and basaltic rock from Vailulu'u Seamount, American Samoa. Geomicrobiol J 26:581–596. https://doi.org/10.1080/01490450903263400.
88. Davis RE, Stakes DS, Wheat CG, Moyer CL. 2009. Bacterial variability within an iron-silica-manganese-rich hydrothermal mound located off-axis at the Cleft Segment, Juan de Fuca Ridge. Geomicrobiol J 26:570–580. https://doi.org/10.1080/01490450902889080.
89. Orcutt BN, Bach W, Becker K, Fisher AT, Hentscher M, Toner BM, Wheat CG, Edwards KJ. 2011. Colonization of subsurface microbial observatories deployed in young ocean crust. ISME J 5:692–703. https://doi.org/10.1038/ismej.2010.157.
90. Handley KM, Boothman C, Mills RA, Pancost RD, Lloyd JR. 2010. Functional diversity of bacteria in a ferruginous hydrothermal sediment. ISME J 4:1193–1205. https://doi.org/10.1038/ismej.2010.38.
91. Meyer-Dombard DAR, Amend JP, Osburn MR. 2012. Microbial diversity

and potential for arsenic and iron biogeochemical cycling at an arsenic rich, shallow-sea hydrothermal vent (Tutum Bay, Papua New Guinea). Chem Geol 348:37–47. https://doi.org/10.1016/j.chemgeo.2012.02.024.
92. Dhillon A, Teske A, Dillon J, Stahl DA, Sogin ML. 2003. Molecular characterization of sulfate-reducing bacteria in the Guaymas Basin. Appl Environ Microbiol 69:2765–2772. https://doi.org/10.1128/AEM.69.5.2765-2772.2003.
93. Davis RE, Moyer CL. 2008. Extreme spatial and temporal variability of hydrothermal microbial mat communities along the Mariana Island Arc and southern Mariana back-arc system. J Geophys Res Solid Earth 113:B08S15. https://doi.org/10.1029/2007JB005413.
94. McAllister SM, Barnett JM, Heiss JW, Findlay AJ, MacDonald DJ, Dow CL, Luther GW, III, Michael HA, Chan CS. 2015. Dynamic hydrologic and biogeochemical processes drive microbially enhanced iron and sulfur cycling within the intertidal mixing zone of a beach aquifer. Limnol Oceanogr 60:329–345. https://doi.org/10.1002/lno.10029.
95. Cao H, Wang Y, Lee OO, Zeng X, Shao Z, Qian P-Y. 2014. Microbial sulfur cycle in two hydrothermal chimneys on the Southwest Indian Ridge. mBio 5(1):e00980-13. https://doi.org/10.1128/mBio.00980-13.
96. Stauffert M, Cravo-Laureau C, Jezequel R, Barantal S, Cuny P, Gilbert F, Cagnon C, Militon C, Amouroux D, Mahdaoui F, Bouyssiere B, Stora G, Merlin F-X, Duran R. 2013. Impact of oil on bacterial community structure in bioturbated sediments. PLoS One 8:e65347. https://doi.org/10.1371/journal.pone.0065347.
97. Dickinson I, Goodall-Copestake W, Thorne MA, Schlitt T, Ávila-Jiménez ML, Pearce DA. 2016. Extremophiles in an Antarctic marine ecosystem. Microorganisms 4:8. https://doi.org/10.3390/microorganisms4010008.
98. Belila A, El-Chakhtoura J, Otaibi N, Muyzer G, Gonzalez-Gil G, Saikaly PE, van Loosdrecht MCM, Vrouwenvelder JS. 2016. Bacterial community structure and variation in a full-scale seawater desalination plant for drinking water production. Water Res 94:62–72. https://doi.org/10.1016/j.watres.2016.02.039.